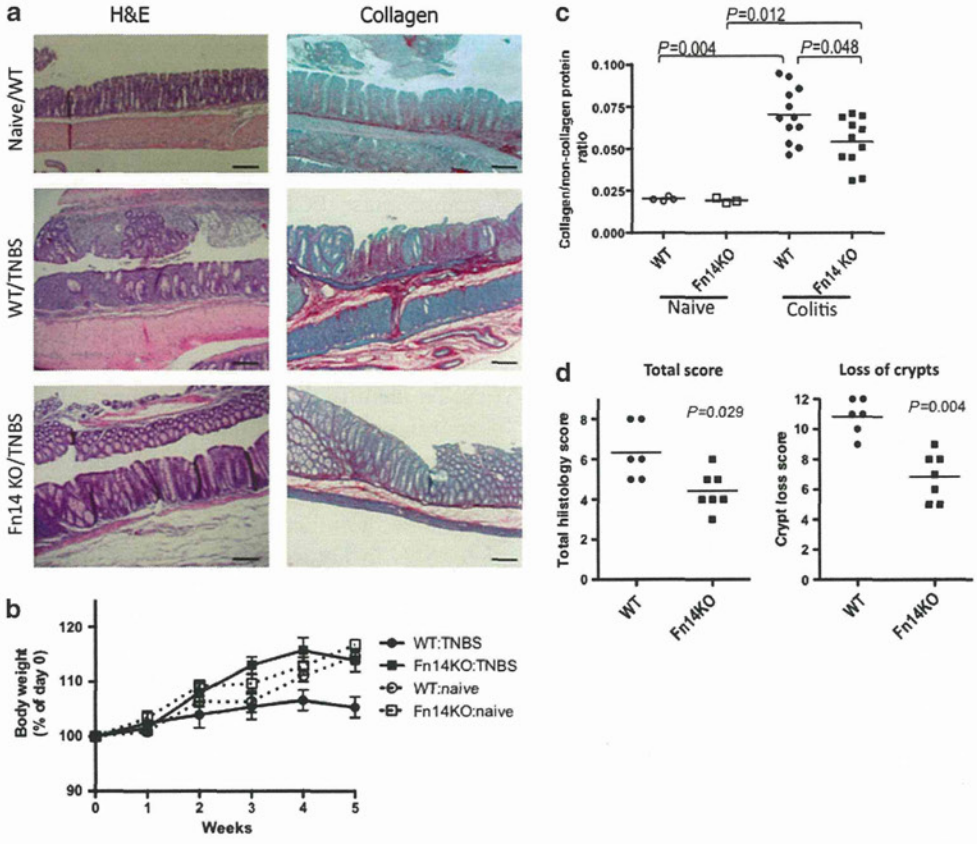

Figure 1 Preserved epithelial cells and less fibrosis in Fn14 (FGF-inducible molecule 14) knockout (KO) mice in chronic colitis. (**a**) After 6 weekly injections of trinitrobenzene sulfonic acid (TNBS), formalin-fixed paraffin-embedded colon sections were prepared for hematoxylin and eosin (H&E) staining (left column) and detection of collagen with Sirius red and non-collagen proteins with fast green (right column). Naive wild-type (WT) is also representative of both naive WT and KO mice. Representative WT and KO with TNBS-induced colitis are shown. Bars = 100 μm. (**b**) Body weight curves of WT or Fn14 KO mice after induction of colitis (WT:TNBS, Fn14 KO:TNBS, $N=9$, respectively). Naive mice ($N=4$) are shown with dotted lines. Data are shown as mean with s.e.m. Difference between WT:TNBS and Fn14 KO:TNBS was statistically significant ($P<0.001$ by two-way analysis of variance analysis). There was no difference between naive WT and FN14 KO mice. (**c**) Ratio of collagen/non-collagen proteins extracted from formalin-fixed paraffin-embedded colon sections prepared from naive or inflamed colon of WT or Fn14 KO mice. (**d**) Scores for total histology and loss of crypts.In **c** and **d**, each dot represents an individual mouse.

characterizes Th1-type responses, is increased in Fn14 KO mice. In addition, the increase in ICOS (inducible costimulator on activated T cells), a hallmark of Th2 cells, and CD69 indicates activated T-cell infiltrates in WT mice but not in KO colons. Most cytokines and chemokines and their receptors, including TGF-β and IL-13Rα2, and connective tissue components and MMPs that were upregulated in WT did not change in Fn14 KO mice as compared with the naive condition, matching the histologically decreased fibrosis and cell infiltration in Fn14 KO mice.

Overall the gene expression profiles support a more prominent Th2-type response and more fibrotic changes with severe inflammation in WT as compared with Fn14 KO mice, mediated by proinflammatory cytokines and chemokines, matrix remodeling enzymes, TGF-β, and IL-13Rα2.

Trinitrophenyl (TNP)-specific immune response was attenuated in Fn14 KO mice with chronic TNBS-induced colitis

As activated T and B cells were involved in the severe inflammation in the WT colon with TNBS-induced colitis and as the expression of genes associated with these adaptive immune cell types altered in KO colon, reflecting reduced Th2-type infiltrates in the KO colon, we investigated the basis for this phenotype. Sacral lymph node (SLN), the draining lymph node of the colon, was swollen after induction of chronic colitis in WT mice, the number of harvested cells was significantly increased in WT as compared with Fn14 KO mice (**Figure 4a**), and a TNP-specific proliferative response was seen in WT but not in Fn14 KO SLN cells (**Figure 4b**). This was surprising as Fn14 is not expressed by T or B cells, and TWEAK/Fn14 pathway deficiency has not previously been shown to affect adaptive immunity.[13]

When cytokine mRNA was measured in pooled fresh SLN cells from WT and Fn14 KO mice with chronic colitis, SLN cells from Fn14 KO mice expressed lower levels of IL-13 transcripts than those of WT mice (**Figure 4c**). No difference was seen in the levels of interferon (IFN)-γ. We also measured the TNP-specific cytokine release by SLN cells and found that IL-2, IL-4, IL-5, IL-6, IL-10, IL-13, and TNF-α were secreted in a TNP-specific manner in WT SLN and were higher in WT than in Fn14 KO mice. IL-12 and IFN-γ were detected without TNBS

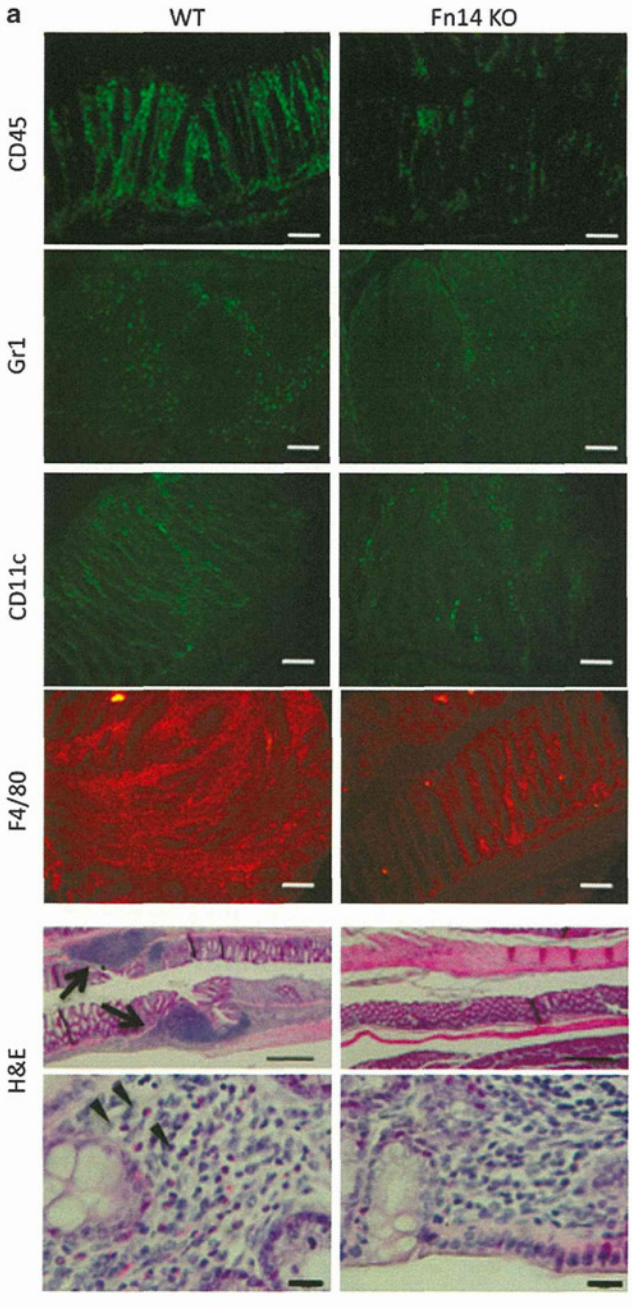

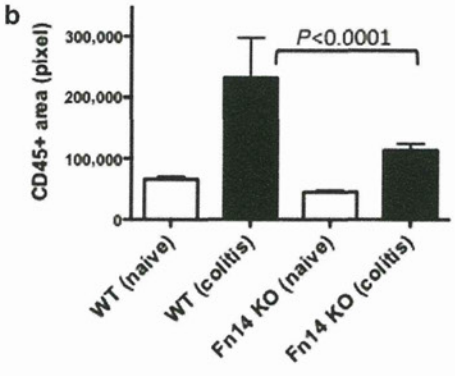

stimuli at comparable levels in SLN cultures from WT and Fn14 KO mice, and statistically significant induction of IL-12 and IFN-γ was not seen in either WT or in KO cultures (**Figure 4d**). IL-17 and IL-25 were also measured but not detected in most of the samples. We further confirmed the cytokine expression of TNP-stimulated SLN cells by quantitative reverse transcriptase–PCR. The level of IL-13 was significantly lower in Fn14 KO mice, while there was no difference in the level of IFN-γ transcripts (**Figure 4e**). These results indicate that a Th2-type TNP-specific immune response with higher production of IL-13 was the major event in WT mice, and it was much attenuated in Fn14 KO mice.

To identify the IL-13-producing cells, we did intracellular staining of IL-13 in mesenteric lymph node (MLN) from WT mice with chronic colitis. Given the relative paucity of cells in SLN, we used MLN cells for the assay after confirming they exhibited a similar cytokine gene expression pattern as reported for SLN in **Figure 4c** (data not shown). Without stimulation, IL-13-producing cells were not detected. With anti-CD3 and anti-CD28 antibody stimulation, IL-13-producing cells were detected within the $CD3^+$ and T-cell receptor-β^+ ($TCR\beta^+$) cells but not in $TCR\gamma\delta^+$ cells or $NKG2D^+$ NK-type cells (**Supplementary Figure S2**). Recently, new IL-13-producing innate cell types were identified.[25–27] To address the possibility that these cell types may produce IL-13, we also stimulated MLN cells with phorbol 12-myristate 13-acetate plus ionomycin and examined $IL\text{-}13^+$ cells in the Lin^-ST2^+ $IL\text{-}7R^+$ or $IL\text{-}7R^-$ subsets. We detected $IL\text{-}13^+$ cells but found them to be very rare (2.73% of the total $IL\text{-}13^+$ cells). Therefore, we conclude that major source of IL-13 in this model is $CD3^+$ T cells.

In order to address whether there was an intrinsic functional defect in IL-13 production as a result of Fn14 deficiency, the MLN cells from WT or Fn14 KO mice were stimulated with anti-CD3/CD28 antibodies. The frequency of $IL\text{-}13^+$ cells was comparable in KO and WT mice (**Figure 5a**) as were the levels of IL-13 released (**Figure 5b**), indicating no such intrinsic defect in Fn14 KO MLN cells. This was also true in case of lamina propria mononuclear cells (LPMC; data not shown). By contrast, restimulation with TNBS induced more $IL\text{-}13^+$ cells

Figure 2 Infiltrating cells in chronic trinitrobenzene sulfonic acid (TNBS)-induced colitis. (**a**) Frozen colon sections from wild-type (WT) and Fn14 (FGF-inducible molecule 14) knockout (KO) mice after 6 weekly injections of TNBS stained with anti-CD45, anti-Gr1, anti-CD11c, or anti-F4/80, to visualize leukocytes, neutrophils, dendritic cells (DC), and macrophages, respectively, show infiltration in both the mucosal and submucosal layers. $CD11c^+$ DCs were mainly in the mucosal layer. All types of cells were localized in the areas of crypt loss and were more abundant in WT colon than in KO tissue. Panels with hematoxylin and eosin (H&E) staining demonstrate the enlargement of colonic patches and eosinophil infiltration at a higher extent in WT mice than Fn14 KO mice. White bars = 100 μm, thick black bars = 500 μm, and thin black bars = 50 μm. Colonic patches and some typical eosinophils infiltrating in lamina propria are indicated with arrows and arrowheads, repectively. (**b**) Total leukocyte cell infiltration determined as $CD45^+$ area. Images as shown in **a** were subjected to image analysis to measure CD45 positive area. Each group included values of three fields from each of six mice.

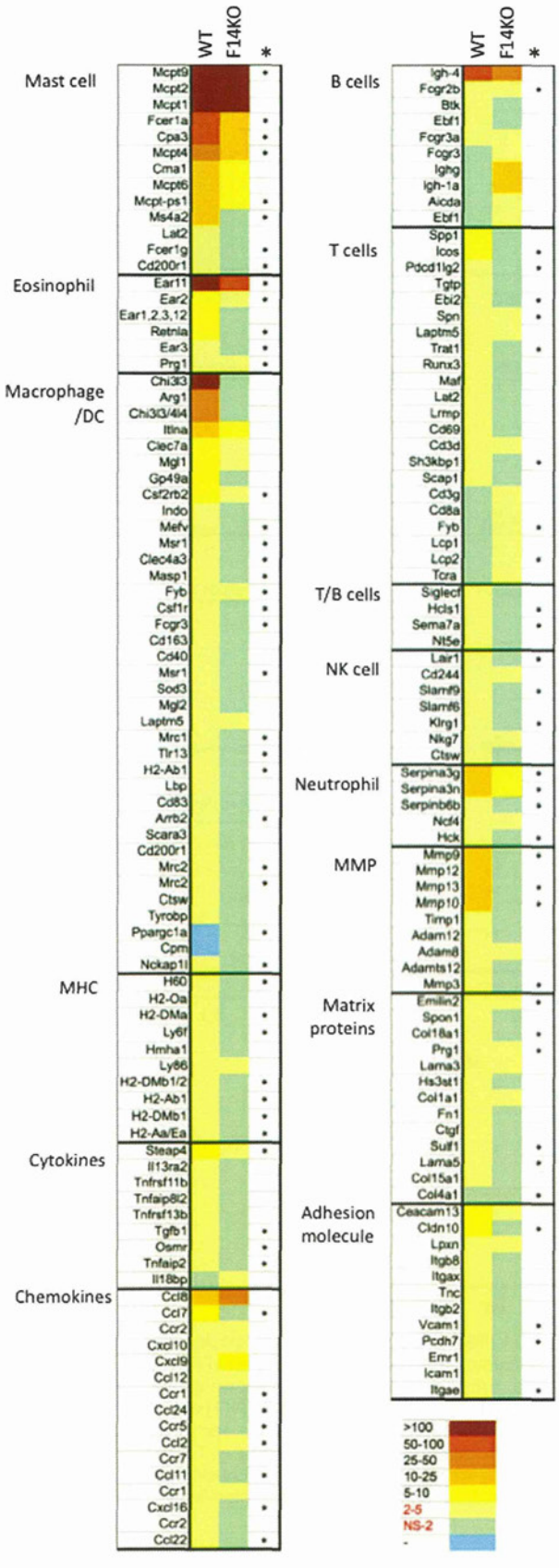

in WT than in Fn14 KO (**Figure 5a**), in agreement with the attenuated Th2 cytokine secretion shown in **Figure 4d**.

Fn14 expression is induced in ECs in chronic TNBS-induced colitis

In order to elucidate the mechanism whereby the TWEAK/Fn14 pathway promoted local inflammation and fibrosis in the colon as well as Th2-type immunity in the draining lymph nodes, we investigated the site of TWEAK/Fn14 pathway expression in TNBS-induced chronic colitis. For this purpose, we separated colon ECs, LPMC and MLN cells from mice with acute stage of colitis (3 day after a rectal injection of TNBS), and chronic phase of colitis (3 days after 6 weekly injections of TNBS) and compared the TWEAK and Fn14 gene expression. To avoid contamination of intraepithelial lymphocytes, ECs were purified as the $EpCAM^{+}CD45^{-}$ cell fraction (**Supplementary Methods** and **Supplementary Figure S1**). Naive mice were compared with mice with acute or chronic stage colitis. In naive mice, TWEAK mRNA expression was higher in naive MLN than LPMC or ECs, whereas the level of Fn14 mRNA in naive mice was very low and comparable in the MLN, LPMC, and intestinal ECs (data not shown). By contrast, TWEAK mRNA was apparently increased in WT ECs at both the acute and chronic time points (**Figure 6a**), although it did not reach statistical difference at chronic time point. A similar pattern of induction of Fn14 mRNA was observed (**Figure 6b**). Neither TWEAK nor Fn14 changed in MLN or LPMC with colitis induction (**Figure 6a,b**). These data support that the TWEAK/Fn14 pathway is upregulated locally in colonic ECs after TNBS-colitis induction and that TWEAK acts through Fn14 on ECs to promote processes underlying Th2-type colitis and fibrosis. They also suggest that TWEAK/Fn14 pathway promotion of Th2-type immunity in the draining nodes is an indirect consequence of its action on ECs within the colon.

Thymic stromal lymphopoietin (TSLP) induction in ECs is reduced in chronic TNBS-induced colitis in Fn14 KO mice.

ECs are a critical innate cell type within the colon that can shape Th2-type immune responses through their production of Th2-driving cytokines, such as TSLP, IL-33, and IL-25.[28,29] Thus TWEAK may act through Fn14 upregulated on ECs to induce their production of these Th2-conditioning cytokines. The levels of TSLP, IL-33, and IL-25 mRNA in ECs from mice before and after colitis induction was measured. We found that ECs had significantly increased TSLP mRNA acutely and chronically after TNBS induction (**Figure 6c**), whereas IL-33 levels

Figure 3 *Gene expression in chronic trinitrobenzene sulfonic acid* (TNBS)-induced colitis in wild-type (WT) and Fn14 (FGF-inducible molecule 14) knockout (KO) colon. Total RNA from whole-colon tissue was harvested from 4–7 mice per experimental group and subjected to microarray analysis. Genes with >two fold change in expression with TNBS as compared with naive tissue are shown for WT and Fn14 KO, with fold change corresponding to the color key, and genes, manually classified according to their gene ontology and cell type expression. Asterisk indicates statistically significant difference between WT and Fn14 KO mice. DC, dendriticells; MHC, major histocompatibility complex; MMP, matrix metalloproteinases; NK, natural killer.

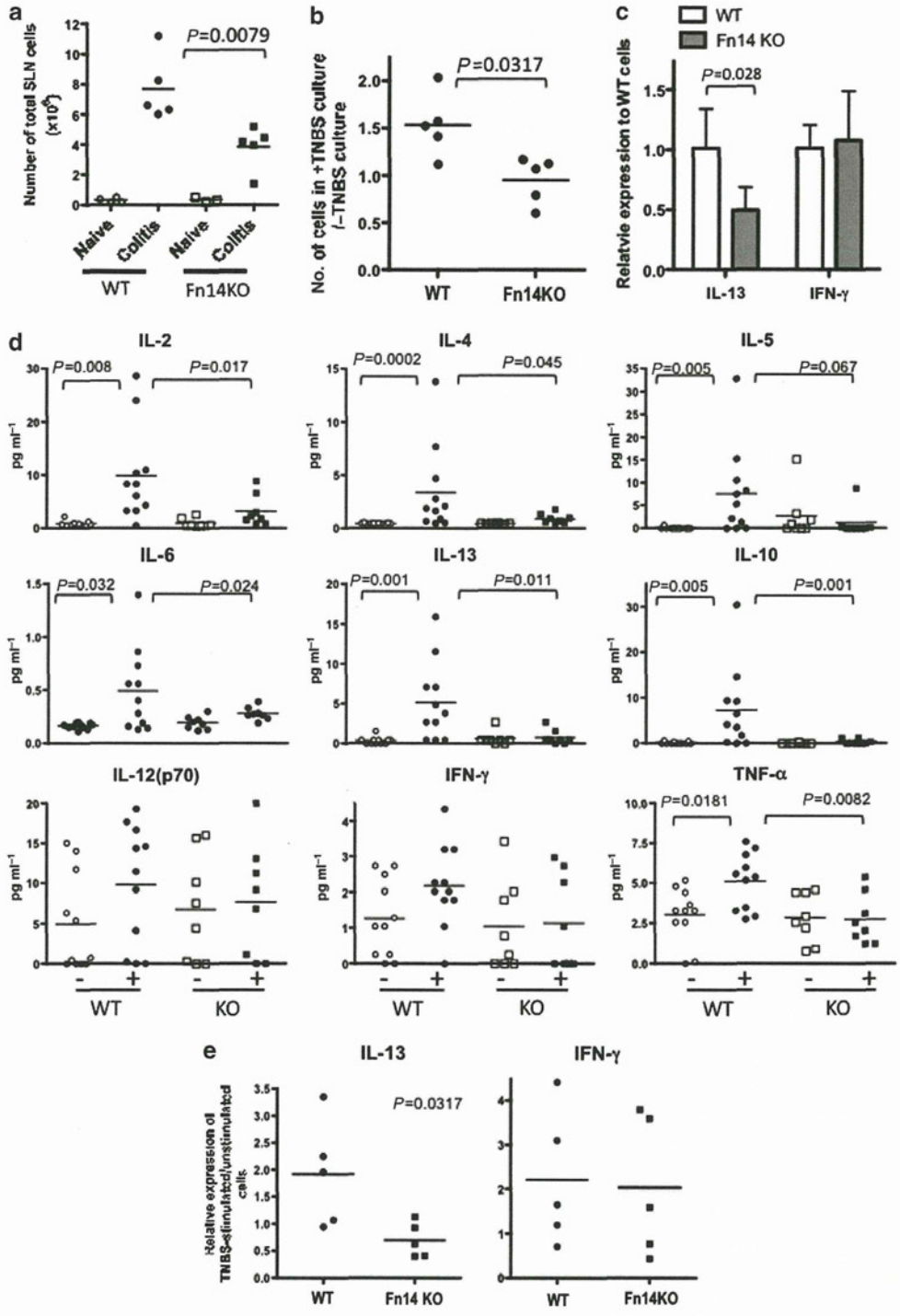

Figure 4 Decreased antigen-specific responses in sacral lymph node (SLN) of Fn14 (FGF-inducible molecule 14) knockout (KO) mice with chronic trinitrobenzene sulfonic acid (TNBS)-induced colitis. (**a**) Number of cells freshly harvested from SLN. (**b**) Trinitrophenyl (TNP)-specific SLN cell proliferation. SLN cells were cultured with or without TNBS and cultured for 2 days. Proliferation response was shown as the ratio of cell number after the culture with TNBS/without TNBS. (**c**) Cytokine mRNA levels of freshly harvested SLN from wild-type (WT) or Fn14 KO ($N=4$ for each group). The quantitative reverse transcriptase–PCR (qRT-PCR) results for interleukin (IL)-13 and interferon (IFN)-γ each expressed relative to WT value defined as one. (**d**) TNP-specific cytokine production in SLN cells. SLN cells were cultured with (+) or without (−) TNBS treatment and culture supernatant was subjected to multiplex cytokine assay. (**e**) TNP-specific cytokine mRNA induction in SLN cells. SLN cells were cultured as in **d** and harvested cells subjected to qRT-PCR for IL-13 or IFN-γ. Each dot represents an individual mouse. Statistically significant *P* values ($P<0.05$) are shown. TNF, tumor necrosis factor.

after induction were marginal and IL-25 levels were not detectable (data not shown). Interestingly, the increase in TSLP mRNA was greater in WT as compared with in Fn14 KO ECs at both stages. Consistent with this, at the level of whole tissue, TSLP was increased 1.7-fold in WT TNBS but not in KO TNBS as compared with their respective naive colons.

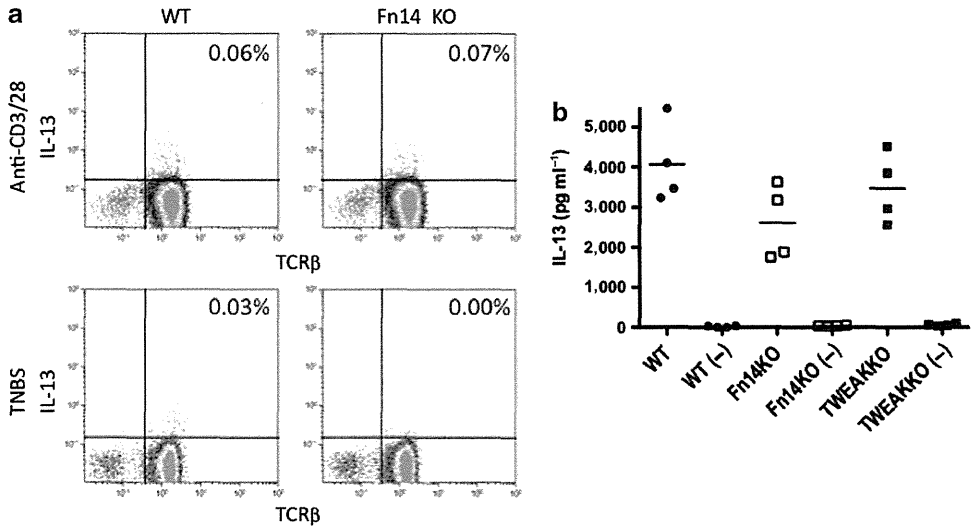

Figure 5 Interleukin (IL)-13 producing cells in mesenteric lymph node (MLN). (**a**) MLN cells from wild-type (WT) or Fn14 (FGF-inducible molecule 14) knockout (KO) mice with chronic colitis were stimulated with anti-CD3 (2 μg ml^{-1} of coating concentration) and anti-CD28 antibody (1 μg ml^{-1}) or trinitrobenzene sulfonic acid (TNBS) and cultured for 48 h. Intracellular staining for IL-13, and surface staining for CD3 and T-cell receptor-β (TCRβ) was performed and results of CD3 gated cells are shown with percentages indicated in the quadrants, representative data of two independent culture of pooled MLN cells from two mice for each genotype. (**b**) MLN cells were stimulated with anti-CD3 antibody and IL-13 secretion was measured. (–) indicates without anti-CD3 antibody. Each symbol indicates an individual mouse. There was no statistically significant difference in WT, Fn14 KO, or TWEAK (tumor necrosis factor (TNF)-like weak inducer of apoptosis) KO-stimulated cells.

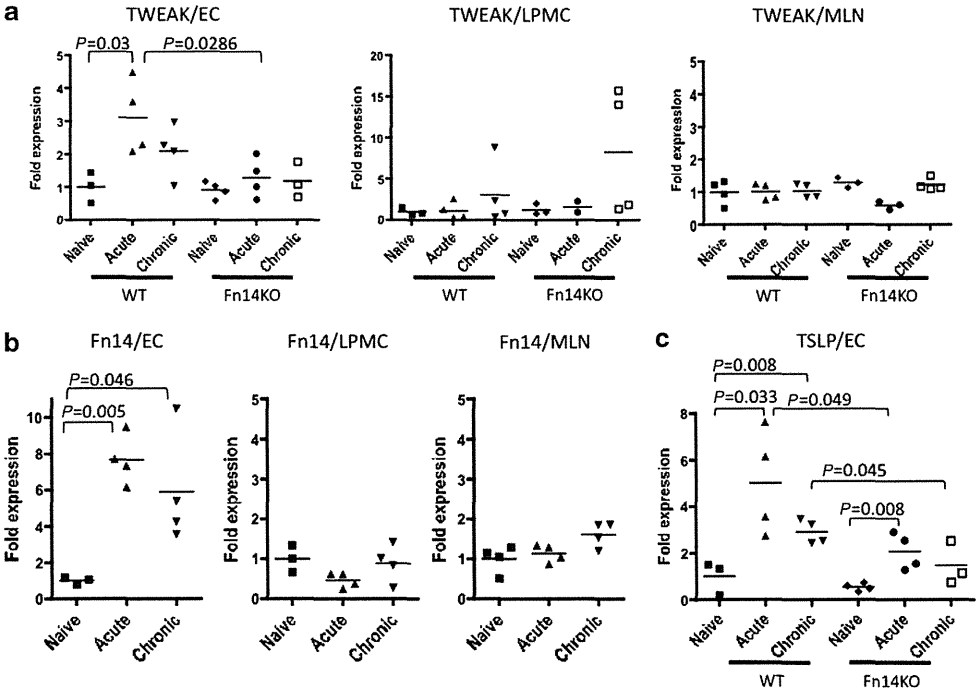

Figure 6 Expression of TWEAK (tumor necrosis factor (TNF)-like weak inducer of apoptosis), Fn14 (FGF-inducible molecule 14), and thymic stromal lymphopoietin (TSLP) in acute and chronic stages of chronic trinitrobenzene sulfonic acid (TNBS)-induced colitis. Gene expression was determined by quantitative reverse transcriptase–PCR using purified epithelial cells (ECs), lamina propria mononuclear cells (LPMC), or mesenteric lymph node (MLN) cells from naive, acute (after single injection of TNBS), and chronic stage (after 6 weekly injections of TNBS) colitis. (**a**) Expression levels of TWEAK in ECs, LPMC, and MLN. (**b**) Expression levels of Fn14 in ECs, LPMC, and MLN. (**c**) Expression levels of TSLP in ECs. In each graph, gene expression levels are expressed relative to the corresponding wild-type (WT) naive sample. Statistically significant *P* values ($P<0.05$) are shown calculated with unpaired *t* test. KO, knockout.

TWEAK induces TSLP expression in ECs in combination with IL-13

We further investigated whether TWEAK acts directly on ECs to induce the expression of TSLP by using naive colon tissue explants. Addition of the TWEAK to the WT colon tissue did not induce alteration of the TSLP mRNA level. As IL-13 was previously shown to upregulate TSLP,[30] we investigated the potential interplay of TWEAK with IL-13 (**Figure 7a**).

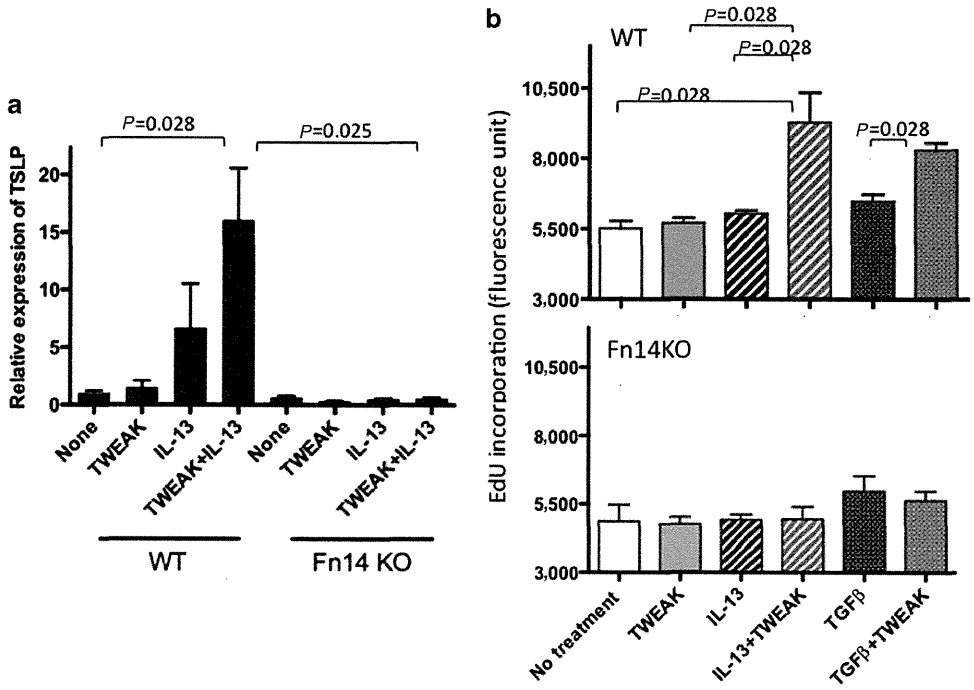

Figure 7 *In vitro* synergistic effect of TWEAK (tumor necrosis factor (TNF)-like weak inducer of apoptosis) and interleuin (IL)-13. (**a**) TWEAK potentiates IL-13-induced expression of thymic stromal lymphopoietin (TSLP) in epithelial cells. Whole-colon tissue from naive wild-type (WT) or Fn14 (FGF-inducible molecule 14) knockout (KO) mice was cultured for 6 h in the presence of TWEAK, IL-13, or both. Total RNA was extracted and TSLP transcripts were measured by quantitative reverse transcriptase–PCR. 'None' indicates control culture without cytokines. Expression levels are shown as relative to WT control culture. (**b**) Mouse embryonic fibroblasts obtained from WT or Fn14 KO BALB/c mice were cultured with TWEAK, IL-13, transforming growth factor-β (TGF-β), or their combination. Cell proliferation was evaluated by the incorporation of EdU (5-ethynyl-2′-deoxyuridine) detected by fluorescence. Data are shown as a mean + s.e.m.

IL-13 showed a trend to upregulate TSLP transcripts but the level did not reach statistically significant difference. Combination of TWEAK and IL-13 strikingly upregulated expression of TSLP, and the difference from control reached a statistically significant level. Importantly, Fn14 KO colon was completely defective in response to TWEAK and IL-13. Therefore, the TWEAK/Fn14 pathway potentiates IL-13-induced TSLP expression. Taken together, these results support that TWEAK promotes Th2-type chronic inflammation and fibrosis by locally inducing EC expression of TSLP.

IL-13 and TWEAK synergistically promote fibroblast proliferation

As fibrosis was decreased in Fn14 KO mice, the direct action of TWEAK on fibroblasts was investigated. Mouse embryonic fibroblasts (MEF) from WT BALB/c mice were obtained and their proliferation assessed (**Figure 7b**). In WT MEF, IL-13 and TGF-β both stimulated MEF proliferation modestly; however, addition of TWEAK greatly enhanced DNA synthesis, especially together with IL-13. These results suggest that TWEAK/Fn14 promotes fibrosis in the presence of IL-13. By contrast, MEF from Fn14 KO mice failed to respond to IL-13 or TWEAK, while their proliferation to TGF-β trended to increase. These results suggest that TWEAK also has a role in supporting the proliferation of fibroblasts, especially in the presence of IL-13.

Chronic colitis with fibrosis was TSLP pathway-dependent.

As the attenuated inflammation and fibrosis in Fn14 KO mice was associated with less TSLP production from ECs, we wished to investigate whether the TSLP pathway has major role in this model, and chronic colitis was induced in TSLPR gene-deficient (TSLPR KO) mice. TSLPR KO mice exhibited a significantly milder colitis as compared with WT mice, very similar to the result in Fn14 KO mice. In comparison with WT mice, histologically less fibrosis was seen (**Figure 8a**), with more body weight gain (**Figure 8b**). Collagen/non-collagen protein ratio was higher in naive TSLPR KO mice than in naive WT mice, but no increase was seen after induction of chronic colitis (**Figure 8c**). They showed a lower total histological score, crypt loss score, and less inflammatory cell infiltration than WT mice (**Figure 8d**). Swelling of SLN was milder than WT mice as shown by the lower numbers of SLN cells, and they did not show evident TNBS-specific proliferative responses (**Figure 8e**). These results indicate that the TSLP pathway has a major role in this model. Finally, addition of exogenous TSLP to LPMC cultures from naive WT or Fn14 KO colon resulted in a similar induction of IL-13 transcripts, suggesting that the decreased IL-13 secretion in Fn14 KO mice described above was due to the reduction in TSLP production by Fn14 KO ECs but not due to a difference in other type of cells (**Figure 8f**).

DISCUSSION

In this study, we show for the first time the role of the TWEAK/Fn14 pathway in a model of chronic fibrotic Th2-type colitis

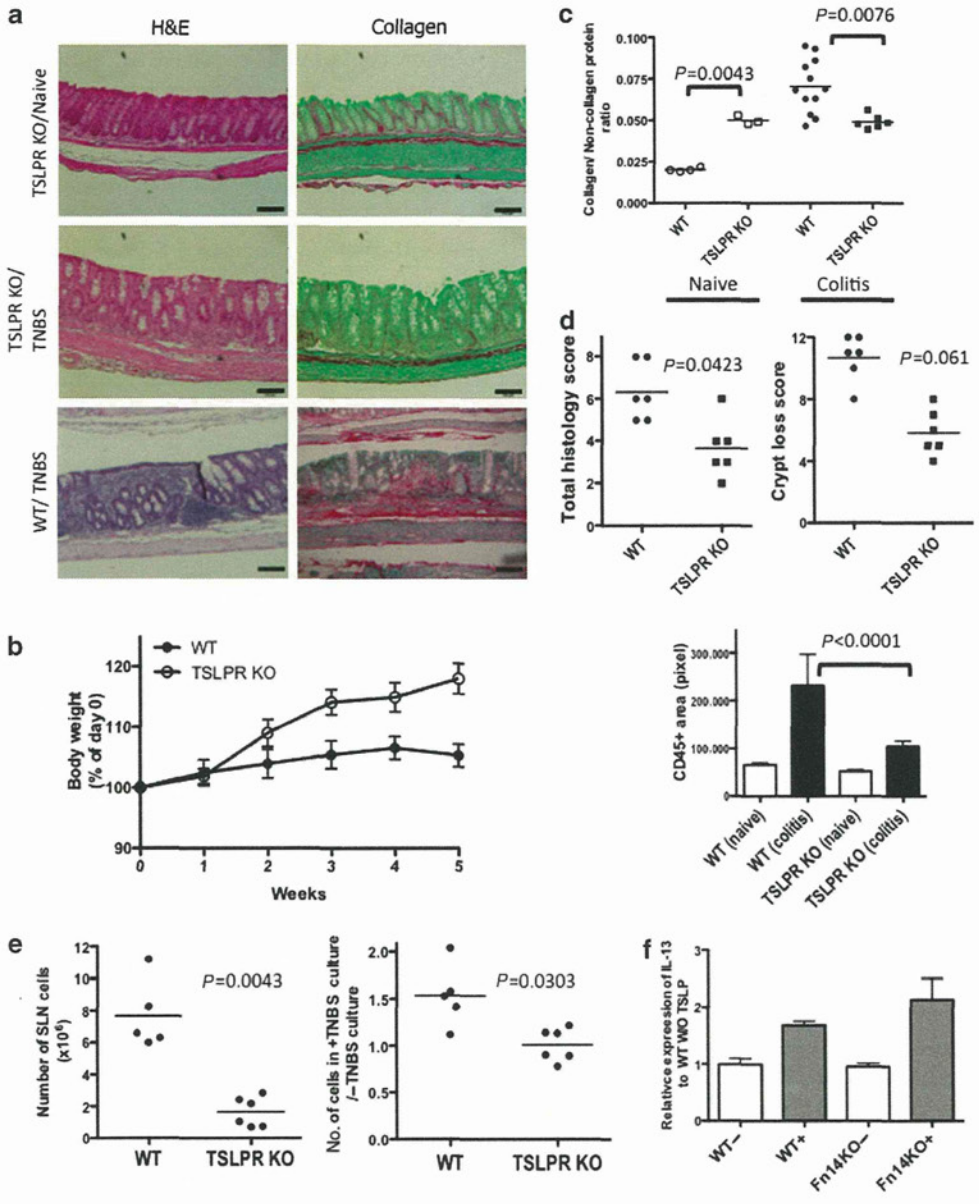

Figure 8 Preserved epithelial cells and less fibrosis in thymic stromal lymphopoietin receptor (TSLPR) knockout (KO) mice in chronic colitis. (**a**) Formalin-fixed paraffin-embedded colon sections from naive or trinitrobenzene sulfonic acid (TNBS)-injected TSLPR KO or wild-type (WT) mice were prepared for hematoxylin and eosin (H&E) staining (left column) and detection of collagen with Sirius red and non-collagen proteins with fast green (right column). Bars = 100 μm. (**b**) Body weight curves of WT or TSLPR KO mice with colitis. Data shown are mean with s.e.m. WT and TSLPR KO group are significantly different ($P<0.001$ by two-way analysis of variance analysis). (**c**) Ratio of collagen to non-collagen proteins extracted from formalin-fixed paraffin-embedded colon sections prepared from naive or inflamed colon of WT or TSLPR KO mice. (**d**) Scores for total histology, crypt loss, and leukocyte infiltration determined as $CD45^+$ area. (**e**) Number of cell yield from freshly harvested sacral lymph node (SLN) and TNBS-specific proliferative responses in WT and TSLPR KO mice determined as described in **Figure 4b**. (**f**) TSLP induced interleukin (IL)-13 mRNA expression in WT and Fn14 (FGF-inducible molecule 14) KO lamina propria mononuclear cells (LPMC). Colon LPMCs obtained from naive WT or Fn14 KO mice were stimulated with TSLP (30 ng ml^{-1}) for 16 h and mRNA of IL-13 quantified. Data are expressed relative to WT without TSLP defined as one as a mean + s.e.m. of three mice for each genotype. In **c**, **d** and **e**, each dot represents an individual mouse. WO, without.

that was previously shown to depend on IL-13. In this model of chronic TNBS-induced colitis, the expression of TWEAK and Fn14 was induced locally in colonic ECs, and deficiency of Fn14 resulted in milder inflammation, tissue damage, and fibrosis than in WT mice. Fn14 KO mice with chronic colitis also exhibited attenuated Th2-type adaptive immune responses in the draining lymph nodes, including reduced IL-13 as compared with WT mice, where the major IL-13-expressing cells were identified as $CD3^+$ $TCR\beta^+$ T cells. However, their lymph node had no intrinsic defect in IL-13 production and little, if any, expression of Fn14, implicating an indirect mechanism of TWEAK signaling through Fn14 in colonic ECs. Further, we elucidate this mechanism by demonstrating Fn14-dependent expression of the Th2-promoting cytokine TSLP by ECs in mice with acute and chronic colitis and TWEAK potentiation of IL-13-induced TSLP in WT colon

explants. Importantly, we show that the TSLP pathway is also required in TNBS-induced chronic colitis, as evidenced by milder disease in TSLPR KO mice similar to that in Fn14 KO mice. Finally, we provide a second mechanism whereby the TWEAK/Fn14 pathway may locally promote fibrotic changes, showing that TWEAK and IL-13 synergize for fibroblast proliferation. Thus our results demonstrate not only the novel role of the TWEAK/Fn14 pathway but also mechanisms whereby it acts in ECs and fibroblasts to promote chronic intestinal inflammation associated with fibrosis.

Fn14 is normally expressed at relatively low levels in healthy tissues[9] but induced by IL-13, TNF-α, or a Toll-like receptor ligand, namely an oligodeoxynucleotide containing CpG motifs in colon mucosa.[10,11] Therefore, with breach of the mucosal barrier with EC damage in colitis, stimuli from bacterial components derived from commensal flora are likely to promote and maintain high expression of Fn14 in the ECs. Indeed, we found that TWEAK and Fn14 were both upregulated in the ECs in TNBS-induced colitis. As TWEAK signaling through Fn14 promotes EC death,[11] it likely further contributes to breakdown of the EC barrier as evidence by the more severe histological scores in WT as compared with Fn14 KO mice. TWEAK/Fn14 signaling in ECs also induces secretion of MMP, cytokines, and chemokines,[10] as shown in our gene profiling, thereby recruiting immune cells, which can also produce TWEAK and signal through the Fn14 upregulated in ECs. Indeed, in this chronic colitis model, chemokines that selectively recruit eosinophils, those for macrophages, and lymphocytes were all significantly higher in WT than Fn14 KO colon after induction of chronic colitis. Thus, the TWEAK/Fn14 pathway exacerbates and perpetuates the colon damage likely by promoting continuous breakdown of the EC barrier and infiltration of immune effector cells.

Although the loss of the intestinal barrier and wide range of exposure to microbial components in the colon are associated with TNBS injection, additionally, as TNBS is a hapten, it induces development of TNP-specific Th2-type adaptive immune responses in the draining lymph nodes and innate and Th2-type adaptive immune cell infiltrates in the colon in WT mice. As this is dependent on IL-13,[19] we identified the major IL-13-expressing cells, which are $CD3^+$ $TCR\beta^+$ T cells with little apparent contribution of innate IL-13-producing cells. In contrast to WT mice, the Fn14 KO exhibited a reduced TNP-specific Th2-type response in the draining lymph nodes, including IL-13 expression, and reduced Th2-type profile shown by histological and gene expression analysis in the colon. This is a novel finding, as previously, little, if any, contribution of TWEAK/Fn14 signaling to systemic acquired immunity was shown in models of collagen-induced arthritis,[14,15] hapten-induced acute colitis,[10] and autoantibody-mediated nephritis induced by chronic graft-vs.-host disease.[16] As the immune response to haptenized lumenal antigen, such as with repeated intrarectal TNBS, may be more enhanced than that in response to antigen administered subcutaneously or directed at target tissues that are relatively sterile, we speculate that this may explain why the TWEAK/Fn14 pathway impacted the adaptive immune response in the draining lymph nodes in chronic colitis but did not have such impact in acute colitis[10] or the other disease models as noted above. Thus, this would constitute an indirect mechanism to explain the reduced TNP-specific response in our current study. Consistent with this, we found little, if any, Fn14 expression in the MLN cells, precluding a direct effect of TWEAK signaling at that site, but rather there is increased expression of Fn14 in the colonic ECs. Thus TWEAK/Fn14 signaling locally in colonic ECs appears to promote a downstream Th2-type response in TNBS-induced chronic colitis in mice.

We further delineated the mechanism whereby Fn14 deficiency reduced the Th2-type response by signaling through Fn14 upregulated in ECs in TNBS-induced chronic colitis. Emerging roles of ECs in bridging the innate immune response and Th2-type immunity have been reported.[28,29] TSLP as well as IL-25 and IL-33 are primary Th2-driving cytokines derived from ECs that act to condition DC, which then leave colon and go to draining nodes and induce/promote Th2-cell responses. Furthermore, recent reports showed that TSLP can induce Th2 cells directly in the absence of antigen-presenting cells.[31–33] In addition, accumulation of mast cells, eosinophils, and basophils in the mucosa of chronic colitis, the cell types known to produce IL-4, IL-5, IL-13, and Th2-cell-recruiting chemokines in response to TSLP,[34–36] contributes to the local amplification of the Th2-type response. IL-13 induces TSLP production from various types of ECs involved in diseases such as airway hypersensitivity, allergic rhinitis and dermatitis, and intestinal parasite infection.[28,29] Notably, we found that the IL-13-induced expression of TSLP in colonic explant cultures is dependent on Fn14 and potentiated by TWEAK. *In vivo,* TSLP, but not IL-25 or IL-33, was significantly increased in WT ECs in acute and chronic TNBS colitis and reduced at both stages in Fn14 KO mice, consistent with their blunted IL-13 response. We also demonstrate that the TSLP pathway is key in this model, as evidenced by milder disease and TNBS-specific responses in TSLPR KO mice, similar to those in Fn14 KO mice. Thus, we propose a mechanistic model in which Fn14 is acutely induced in ECs after TNBS-induced damage, enabling TWEAK to promote EC expression of TSLP acutely in WT but not in Fn14-deficient mice, thereby driving the development of Th2-type immunity, including the expression of IL-13.

Consistent with our model, we found no intrinsic defect in IL-13 expression as a result of Fn14 deficiency, in that WT and Fn14 KO LPMC respond similarly to TSLP, and WT and Fn14 KO draining lymph node cells and LPMC respond similarly to non-specific stimuli. Thus our proposed mechanism, an IL-13-TWEAK/Fn14-TSLP axis in ECs, constitutes a feedforward loop exacerbating and sustaining the chronic Th2-driven TNBS-induced colitis. The detailed mechanism as to how the TWEAK/Fn14 signaling promotes IL-13-induced TSLP expression remains to be investigated. We suggest several possibilities that are not mutually exclusive. As TSLP promoter activation is mediated by an upstream NF-κB site,[37] it is possible that TSLP expression was promoted through NF-κB activation by TWEAK/Fn14 pathway.[38,39] Secondly, as

IL-13 and TWEAK in concert activate endogenous TNF-α,[11] the induction of TSLP expression may be mediated by TNF-α, which is also known to promote TSLP expression in ECs.[37]

Another important point in our study is the link between the TWEAK/Fn14 pathway and fibrosis. Although not yet reported in the context of colitis, studies from multiple other systems have indicated a role for TWEAK/Fn14 in driving fibrogenic responses. For example, TWEAK/Fn14 dependence of collagen deposition has been reported in the liver injury,[40] kidney after ischemia reperfusion injury,[41] skeletal muscle in a model of denervation-induced skeletal muscle atrophy,[42] and heart in the context of dilated cardiomyopathy.[43] Although the TWEAK/Fn14 pathway may drive fibrosis through its promotion of chronic inflammatory activity, particularly Th2-type activity, there are also accumulating evidence supporting that the TWEAK/Fn14 pathway contribute to fibrosis through its direct action on fibroblasts/myofibroblasts and their progenitors. As Fn14 is upregulated by TGF-β on fibroblasts,[44,45] and is likely also expressed on myofibroblasts, the TWEAK/Fn14 pathway may directly contribute to a fibrogenic response by regulating the proliferation of these fibroblasts, their differentiation to myofibroblasts, and extracellular matrix production. Indeed, our current study shows that TWEAK synergizes with IL-13 or TGF-β to promote the expansion of fibroblasts, and this is dependent on Fn14.

Thus, the TWEAK/Fn14 pathway is involved together with IL-13 in mediating an IL-13-TWEAK/Fn14-TSLP axis in ECs, as well as through its interplay with IL-13 and TGF-β in fibroblasts, to aggravate and perpetuate Th2-type chronic inflammation with fibrosis. As fibrosis is associated with fistula and stricture formation in Crohn's disease and there is widespread damage of mucosa in ulcerative colitis, we propose that targeting TWEAK/Fn14 as possible treatment of inflammatory bowel diseases. Our findings also have interesting implications, warranting investigation of a role for the TWEAK/Fn14 pathway in other diseases involving ECs and prominent roles for IL-13, TSLP, and fibrotic changes, such as chronic respiratory and skin diseases.

METHODS

Mice. Female 7-week-old BALB/c mice or Fn14 KO mice[46] with BALB/c background were used. All experimental protocols were approved by the local institutional animal care and use committees of the National Center for Global Health and Medicine, Japan. TSLP receptor–deficient (TSLPR KO) mice were generated as described previously[47] and backcrossed to BALB/c for 12 generations.

Induction of TNBS colitis. To induce chronic colitis, under anesthesia with ketamine and xylazine, 0.2% TNBS (Research Organics, Cleveland, OH) in phosphate-buffered saline: ethanol = 1:1 was rectally injected with a stainless gavage tube weekly for 6 consecutive weeks, with modification of a previously reported method.[21] The dose of TNBS solution was sequentially increased: 1.0, 1.5, 1.5, 1.8, 2.0, and 2.0 μl per g body weight. Tissues and cells were harvested 3 days after the last injection. To induce acute colitis, mice were injected with 1.0 μl per g body weight on day 0, and tissues were obtained on day 3. The colon was opened longitudinally, rolled, and snap frozen for preparation of frozen sections or RNA extraction. In some experiments, formalin-fixed paraffin-embedded sections were prepared for hematoxylin and eosin staining or detection of collagen (**Supplementary Methods**). Collagen and non-collagen proteins of tissue sections were measured using a Quantitative Micro-Assay Kit for Collagen and Non-Collagen Proteins (Chondrex, Redmond, WA) following the vendor's protocol.

Total RNA purification, gene profiling and quantitative reverse transcriptase–PCR. Total RNA was extracted and purified with DNAse. After reverse transcription, expression level of each gene was quantified using TaqMan gene expression kit (ABI, Carlsbad, CA) or a SYBR Green PCR Master Mix. For gene profiling, RNA was isolated from snap-frozen whole-colon tissues, including five naive WT mice, five naive Fn14 KO mice, six WT mice, and seven Fn14 KO with repeated TNBS-induced colitis and subjected to gene profiling performed with automated probe labeling, hybridization, and scanning as previously described.[10] Details for the reverse transcriptase–PCR and analysis of Affymetrix data are as described in **Supplementary Methods**.

Primary tissue culture. The mouse colon tissues were washed with phosphate-buffered saline and cut into 1-cm lengths, opened, placed in 24-well plates, and kept in RPMI 1640 with 5% fetal calf serum, Tissues were then cultured with 50 ng ml^{-1} of recombinant IL-13 (PeproTech, Rocky Hill, NJ) or 100 ng ml^{-1} of recombinant soluble TWEAK (prepared by Biogen Idec, Cambridge, MA)[3] at 37 °C, 5% CO_2 for 6 h. The tissues were frozen in liquid nitrogen and stored at −80°C until use.

Statistical analysis. Data were statistically analyzed by the Mann–Whitney test using a software Prism 4 (GraphPad Software, La Jolla, CA), unless indicated in the legend.

Methods for histological analysis, cell separation, cell culture, and cytokine quantification are described in the **Supplementary information**.

SUPPLEMENTARY MATERIAL is linked to the online version of the paper at http://www.nature.com/mi

ACKNOWLEDGEMENTS

We are grateful to Dr Suzanne Szak (Biogen Idec) for valuable review and suggestions on this manuscript, Mr Yasuhiko Nagasaka (Beckman Coulter) for his help with flow cytometric analysis and Dr M Tamura-Nakano (NCGM EM Support Unit) for her technical support for histological analysis. *Grant support:* This work was supported partly by grants and contracts from the program Grants-in-Aid for Scientific Research (B and C) and Grants-in Aid for Young Scientists (B) from the Ministry of Education, Cultures, Sports, Science, and Technology; Japan Science and Technology Agency; The Grant of National Center for Global Health and Medicine (21-110, 22-205); and Grants for Research on New Drugs Development and Research on intractable diseases from Ministry of Health, Labor and Welfare of Japan. *Transcripts profiling:* The microarray files and information have been uploaded to the NCBI GEO public repository (accession number GSE36806).

DISCLOSURE

Ping Wu, and Linda C. Burkly are employees and stockholders in Biogen Idec. All the other authors declared no conflict of interest.

REFERENCES

1. Fichtner-Feigl, S., Strober, W., Geissler, E.K. & Schlitt, H.J. Cytokines mediating the induction of chronic colitis and colitis-associated fibrosis. *Mucosal immunol.* **1** (Suppl 1), S24–S27 (2008).
2. Wynn, T.A. & Ramalingam, T.R. Mechanisms of fibrosis: therapeutic translation for fibrotic disease. *Nat Med.* **18**, 1028–1040 (2012).

3. Chicheportiche, Y. *et al.* TWEAK, a new secreted ligand in the tumor necrosis factor family that weakly induces apoptosis. *J. Biol. Chem.* **272**, 32401–32410 (1997).
4. Kaplan, M.J. *et al.* The apoptotic ligands TRAIL, TWEAK, and Fas ligand mediate monocyte death induced by autologous lupus T cells. *J. Immunol.* **169**, 6020–6029 (2002).
5. Maecker, H. *et al.* TWEAK attenuates the transition from innate to adaptive immunity. *Cell* **123**, 931–944 (2005).
6. Nakayama, M. *et al.* Fibroblast growth factor-inducible 14 mediates multiple pathways of TWEAK-induced cell death. *J. Immunol.* **170**, 341–348 (2003).
7. Justo, P. *et al.* Cytokine cooperation in renal tubular cell injury: the role of TWEAK. *Kidney Int.* **70**, 1750–1758 (2006).
8. Burkly, L.C., Michaelson, J.S. & Zheng, T.S. TWEAK/Fn14 pathway: an immunological switch for shaping tissue responses. *Immunol. Rev.* **244**, 99–114 (2011).
9. Winkles, J.A. The TWEAK-Fn14 cytokine-receptor axis: discovery, biology and therapeutic targeting. *Nat. Rev. Drug Discov.* **7**, 411–425 (2008).
10. Dohi, T. *et al.* TWEAK/Fn14 pathway: a nonredundant role in intestinal damage in mice through a TWEAK/intestinal epithelial cell axis. *Gastroenterology* **136**, 912–923 (2009).
11. Kawashima, R. *et al.* Interleukin-13 damages intestinal mucosa via TWEAK and Fn14 in mice—a pathway associated with ulcerative colitis. *Gastroenterology* **141**, 2119–2129 (2011).
12. Burkly, L.C. & Dohi, T. The TWEAK/Fn14 pathway in tissue remodeling: for better or for worse. *Adv. Exp. Med. Biol.* **691**, 305–322 (2011).
13. Zheng, T.S. & Burkly, L.C. No end in site: TWEAK/Fn14 activation and autoimmunity associated- end-organ pathologies. *J. Leukoc. Biol.* **84**, 338–347 (2008).
14. Perper, S.J. *et al.* TWEAK is a novel arthritogenic mediator. *J. Immunol.* **177**, 2610–2620 (2006).
15. Kamata, K. *et al.* Involvement of TNF-like weak inducer of apoptosis in the pathogenesis of collagen-induced arthritis. *J. Immunol.* **177**, 6433–6439 (2006).
16. Zhao, Z. *et al.* TWEAK/Fn14 interactions are instrumental in the pathogenesis of nephritis in the chronic graft-versus-host model of systemic lupus erythematosus. *J. Immunol.* **179**, 7949–7958 (2007).
17. Wilson, M.S. & Wynn, T.A. Pulmonary fibrosis: pathogenesis, etiology and regulation. *Mucosal Immunol.* **2**, 103–121 (2009).
18. Ingram, J.L. *et al.* Opposing actions of Stat1 and Stat6 on IL-13-induced up-regulation of early growth response-1 and platelet-derived growth factor ligands in pulmonary fibroblasts. *J. Immunol.* **177**, 4141–4148 (2006).
19. Fichtner-Feigl, S. *et al.* Induction of IL-13 triggers TGF-beta1-dependent tissue fibrosis in chronic 2,4,6-trinitrobenzene sulfonic acid colitis. *J. Immunol.* **178**, 5859–5870 (2007).
20. Wu, F. & Chakravarti, S. Differential expression of inflammatory and fibrogenic genes and their regulation by NF-kappaB inhibition in a mouse model of chronic colitis. *J. Immunol.* **179**, 6988–7000 (2007).
21. Lawrance, I.C. *et al.* A murine model of chronic inflammation-induced intestinal fibrosis down-regulated by antisense NF-kappa B. *Gastroenterology* **125**, 1750–1761 (2003).
22. Gordon, S. & Martinez, F.O. Alternative activation of macrophages: mechanism and functions. *Immunity* **32**, 593–604 (2010).
23. Pemberton, A.D. *et al.* Innate BALB/c enteric epithelial responses to *Trichinella spiralis*: inducible expression of a novel goblet cell lectin, intelectin-2, and its natural deletion in C57BL/10 mice. *J. Immunol.* **173**, 1894–1901 (2004).
24. Gu, N. *et al.* Intelectin is required for IL-13-induced monocyte chemotactic protein-1 and -3 expression in lung epithelial cells and promotes allergic airway inflammation. *Am. J. Physiol. Lung. Cell. Mol. Physiol.* **298**, L290–L296 (2010).
25. Moro, K. *et al.* Innate production of T(H)2 cytokines by adipose tissue-associated c-Kit(+)Sca-1(+) lymphoid cells. *Nature* **463**, 540–544 (2010).
26. Neill, D.R. *et al.* Nuocytes represent a new innate effector leukocyte that mediates type-2 immunity. *Nature* **464**, 1367–1370 (2010).
27. Saenz, S.A. *et al.* IL25 elicits a multipotent progenitor cell population that promotes T(H)2 cytokine responses. *Nature* **464**, 1362–1366 (2010).
28. Bulek, K., Swaidani, S., Aronica, M. & Li, X. Epithelium: the interplay between innate and Th2 immunity. *Immunol. Cell. Biol.* **88**, 257–268 (2010).
29. Saenz, S.A., Taylor, B.C. & Artis, D. Welcome to the neighborhood: epithelial cell-derived cytokines license innate and adaptive immune responses at mucosal sites. *Immunol. Rev.* **226**, 172–190 (2008).
30. Biton, M. *et al.* Epithelial microRNAs regulate gut mucosal immunity via epithelium-T cell crosstalk. *Nat. Immunol.* **12**, 239–246 (2011).
31. Blazquez, A.B., Mayer, L. & Berin, M.C. Thymic stromal lymphopoietin is required for gastrointestinal allergy but not oral tolerance. *Gastroenterology* **139**, 1301–1309 (2010).
32. He, R. *et al.* TSLP acts on infiltrating effector T cells to drive allergic skin inflammation. *Proc. Natl. Acad. Sci. USA* **105**, 11875–11880 (2008).
33. Omori, M. & Ziegler, S. Induction of IL-4 expression in CD4(+) T cells by thymic stromal lymphopoietin. *J. Immunol.* **178**, 1396–1404 (2007).
34. Allakhverdi, Z. *et al.* Thymic stromal lymphopoietin is released by human epithelial cells in response to microbes, trauma, or inflammation and potently activates mast cells. *J. Exp. Med.* **204**, 253–258 (2007).
35. Allakhverdi, Z., Smith, D.E., Comeau, M.R. & Delespesse, G. Cutting edge: The ST2 ligand IL-33 potently activates and drives maturation of human mast cells. *J. Immunol.* **179**, 2051–2054 (2007).
36. Siracusa, M.C. *et al.* TSLP promotes interleukin-3-independent basophil haematopoiesis and type 2 inflammation. *Nature* **477**, 229–233 (2011).
37. Lee, H.C. & Ziegler, S.F. Inducible expression of the proallergic cytokine thymic stromal lymphopoietin in airway epithelial cells is controlled by NFkappaB. *Proc. Natl. Acad. Sci. USA* **104**, 914–919 (2007).
38. Brown, S.A., Ghosh, A. & Winkles, J.A. Full-length, membrane-anchored TWEAK can function as a juxtacrine signaling molecule and activate the NF-kappaB pathway. *J. Biol. Chem.* **285**, 17432–17441 (2010).
39. Roos, C. *et al.* Soluble and transmembrane TNF-like weak inducer of apoptosis differentially activate the classical and noncanonical NF-kappa B pathway. *J. Immunol.* **185**, 1593–1605 (2010).
40. Tirnitz-Parker, J.E. *et al.* Tumor necrosis factor-like weak inducer of apoptosis is a mitogen for liver progenitor cells. *Hepatology* **52**, 291–302 (2010).
41. Hotta, K. *et al.* Direct targeting of fibroblast growth factor-inducible 14 protein protects against renal ischemia reperfusion injury. *Kidney Int.* **79**, 179–188 (2011).
42. Mittal, A. *et al.* The TWEAK-Fn14 system is a critical regulator of denervation-induced skeletal muscle atrophy in mice. *J. Cell. Biol.* **188**, 833–849 (2010).
43. Jain, M. *et al.* A novel role for tumor necrosis factor-like weak inducer of apoptosis (TWEAK) in the development of cardiac dysfunction and failure. *Circulation* **119**, 2058–2068 (2009).
44. Hosokawa, Y., Hosokawa, I., Ozaki, K., Nakae, H. & Matsuo, T. Proinflammatory effects of tumour necrosis factor-like weak inducer of apoptosis (TWEAK) on human gingival fibroblasts. *Clin. Exp. Immunol.* **146**, 540–549 (2006).
45. Meighan-Mantha, R.L. *et al.* The mitogen-inducible Fn14 gene encodes a type I transmembrane protein that modulates fibroblast adhesion and migration. *J. Biol. Chem.* **274**, 33166–33176 (1999).
46. Jakubowski, A. *et al.* TWEAK induces liver progenitor cell proliferation. *J. Clin. Invest.* **115**, 2330–2340 (2005).
47. Carpino, N. *et al.* Absence of an essential role for thymic stromal lymphopoietin receptor in murine B-cell development. *Mol. Cell. Biol.* **24**, 2584–2592 (2004).

nature COMMUNICATIONS

ARTICLE

Received 7 Sep 2012 | Accepted 28 Feb 2013 | Published 3 April 2013

DOI: 10.1038/ncomms2668

Microbiota-derived lactate accelerates colon epithelial cell turnover in starvation-refed mice

Toshihiko Okada[1,2], Shinji Fukuda[3,4,†], Koji Hase[4,5,†], Shin Nishiumi[6], Yoshihiro Izumi[6], Masaru Yoshida[6,7], Teruki Hagiwara[1], Rei Kawashima[1,†], Motomi Yamazaki[1], Tomoyuki Oshio[1,†], Takeshi Otsubo[1], Kyoko Inagaki-Ohara[1], Kazuki Kakimoto[1,2], Kazuhide Higuchi[2], Yuki I. Kawamura[1], Hiroshi Ohno[3,4] & Taeko Dohi[1,8]

Oral food intake influences the morphology and function of intestinal epithelial cells and maintains gastrointestinal cell turnover. However, how exactly these processes are regulated, particularly in the large intestine, remains unclear. Here we identify microbiota-derived lactate as a major factor inducing enterocyte hyperproliferation in starvation-refed mice. Using bromodeoxyuridine staining, we show that colonic epithelial cell turnover arrests during a 12- to 36-h period of starvation and increases 12–24 h after refeeding. Enhanced epithelial cell proliferation depends on the increase in live *Lactobacillus murinus*, lactate production and dietary fibre content. In the model of colon tumorigenesis, mice exposed to a carcinogen during refeeding develop more aberrant crypt foci than mice fed *ad libitum*. Furthermore, starvation after carcinogen exposure greatly reduced the incidence of aberrant crypt foci. Our results indicate that the content of food used for refeeding as well as the timing of carcinogen exposure influence the incidence of colon tumorigenesis in mice.

[1] Department of Gastroenterology, Research Center for Hepatitis and Immunology, Research Institute, National Center for Global Health and Medicine, 1-7-1 Kohnodai, Ichikawa, Chiba 272-8516, Japan. [2] Second Department of Internal Medicine, Osaka Medical College, 2-7 Daigakumachi, Takatsuki, Osaka 569-8686, Japan. [3] Laboratory for Epithelial Immunobiology, RIKEN Research Center for Allergy and Immunology, 1-7-22 Suehiro-cho, Tsurumi-ku, Yokohama, Kanagawa 230-0045, Japan. [4] Graduate School of Nanobioscience, Yokohama City University, 1-7-29 Suehiro-cho, Tsurumi-ku, Yokohama, Kanagawa 230-0045, Japan. [5] Bioenvironmental Epigenetics, 1-7-22 Suehiro-cho, Tsurumi-ku, Yokohama, Kanagawa 230-0045, Japan. [6] Division of Gastroenterology, Department of Internal Medicine, Kobe University Graduate School of Medicine, 7-5-1 Kusunoki-cho, Chuo-ku, Kobe, Hyogo 650-0017, Japan. [7] Division of Metabolomics Research, Department of Internal Medicine, Kobe University Graduate School of Medicine, 7-5-1 Kusunoki-cho, Chuo-ku, Kobe, Hyogo 650-0017, Japan. [8] Open Laboratory for Allergy Research, RIKEN Research Center for Allergy and Immunology, 1-7-22 Suehiro-cho, Tsurumi-ku, Yokohama, Kanagawa 230-0045, Japan. † Present addresses: Institute for Advanced Biosciences, Keio University, 246-2 Mizukami, Kakuganji, Tsuruoka, Yamagata 997-0052, Japan (S.F); Division of Mucosal Barriology, The Institute of Medical Science, The University of Tokyo, 4-6-1 Shirokanedai, Minato-ku, Tokyo 108-8639, Japan (K.H); Kitasato University Graduate School of Medical Sciences, 1-15-1 Kitasato, Minami-ku, Sagamihara, Kanagawa 252-0373, Japan (R.K); Department of Dermatology, Jichi Medical University, 3311-1 Yakushiji, Shimotsuke, Tochigi 329-0498, Japan (T.O). Correspondence and requests for materials should be addressed to T.D. (email: dohi@ri.ncgm.go.jp).

The gastrointestinal (GI) tract must adapt to drastic changes in the lumenal environment to maintain homoeostasis, and responses to ingested food are the most fundamental physiological adaptations. Epithelial cells (EC) in the GI tract undergo rapid self-renewal, with a new gut lining produced approximately every 3 days[1]. However, the turnover rate is not always constant. For example, gut EC proliferation rates undergo circadian fluctuation in rodents[2,3] and humans[4,5], which alters the morphology and function of the GI tract. In the normal human rectal biopsies, ^{3}H-thymidine incorporation into cells is higher at night and lower in the afternoon[5]. This circadian rhythm is controlled by clock genes in the central nervous system, as well as local expression of clock genes in intestinal tissue. EC proliferation rates also vary in a longer time span. For example, the GI tract of animals becomes atrophic during hibernation but undergoes rapid recovery on food intake after hibernation[6,7]. To illustrate, snakes usually eat after starvation of several months. On food intake, the snake intestine doubles in wet and dry mass within 1 day, largely as a result of a sixfold increase in microvillus length and a doubling of mucosal EC volume[8]. Thus, oral food intake should greatly change the rate of intestinal cell turnover. In nocturnal rodents, daytime feeding is a strong synchronizer of GI clock genes[9]. In rats, starvation reduces the weight and thickness of the small intestine[10]. In humans, total parenteral nutrition causes atrophy of intestinal mucosa[11,12]. Therefore, oral food intake is necessary for maintenance of cell proliferation and has the highest impact on the morphology and function of the GI tract. However, the mechanisms underlying how food intake regulates EC proliferation are not fully elucidated. In particular, there are few reports about how food intake affects colonic EC proliferation.

Colonic EC turnover is slower than cell turnover in the small intestine. One reason may be the major difference in the luminal environments of the small and large intestines. Nutrients are mostly digested and absorbed in the small intestine, whereas the colon is colonized by microbiota. Thus, instead of orally ingested nutrients taken in by the host, the colon lumen is rich in microbial metabolites and fermentation products produced by the microbiota. As a result, colonic EC rely heavily on fermentation products of intestinal microorganisms, including butyric acid, as a source of carbon and energy[13]. The quality of nutrients for colonic EC is thus associated with the microbiota 'enterotype'[14,15] of the host and may also be associated with the incidence of diseases in the GI tract, including colorectal cancer, as well as diseases affecting other organs[16].

In this study, we found that starvation arrested colon EC turnover, and refeeding induced hyperproliferation in mice. The enhanced EC proliferation was dependent on the microbiota, more specifically lactobacilli and their metabolite lactic acid, which likely supported energy production in EC. We also found that this shift of EC turnover rate by starvation-refeeding dramatically changed the susceptibility to carcinogen exposure.

Results

Transient proliferation of colonic EC in refed mice. We first evaluated the EC turnover of the small and large intestines on starvation and refeeding by quantifying bromodeoxyuridine (BrdU) incorporation into EC. After 36 h of starvation, the number of BrdU + cells in both the small intestine and colon was less than in non-starved controls (Supplementary Fig. S1a), but the difference was only statistically significant in the colon (Fig. 1a,b). Cell turnover in the small intestine recovered to the level of non-starved control mice by 2 h after refeeding. In contrast, in the colon, recovery of cell proliferation was not seen until 6 h after refeeding; thereafter, proliferation exceeded control levels by approximately threefold at 12 h. This excessive cell proliferation continued for 24 h and returned to basal levels by 76 h after refeeding (Fig. 1). In spite of the increased number of proliferating cells, there was no apparent change in the thickness

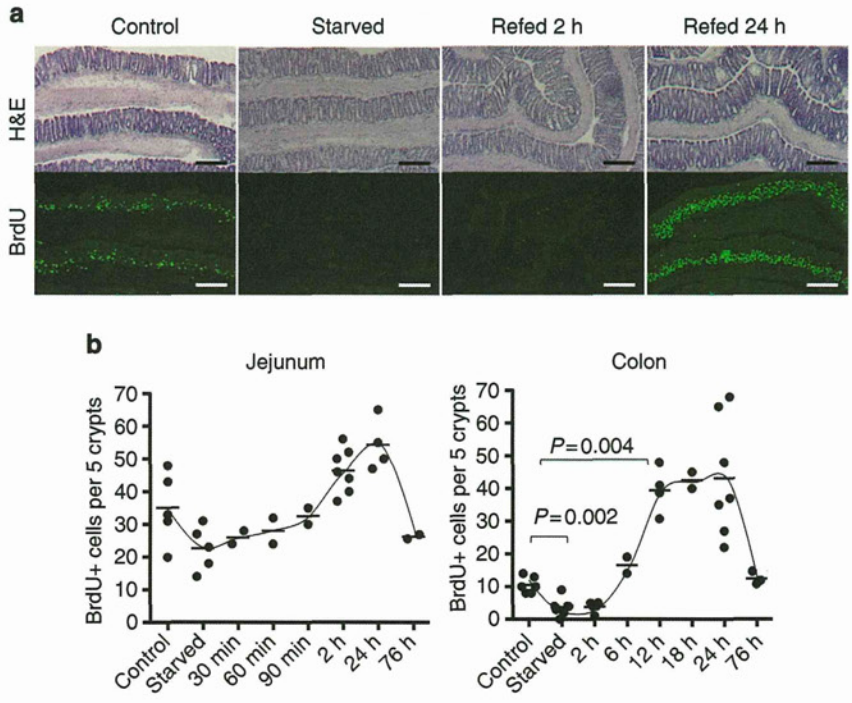

Figure 1 | Starvation-refeeding induced transient colonic EC hyperproliferation. (**a**) Colonic tissues were taken from mice fed *ad libitum* (control), mice starved for 36 h and mice starved for 36 h and refed with normal bait (CE2) for 2 or 24 h. Frozen sections were stained with hematoxylin and eosin (H&E; upper) and anti-BrdU antibody (lower, green). Scale bar, 200 μm. (**b**) Number of BrdU + cells per five crypts was counted at each time point. Each dot indicates an individual mouse. Mann–Whitney test was performed for *P*-value.

of the colonic mucosa. However, the frequency of apoptosis detected with terminal deoxynucleotidyl transferase dUTP nick-end labelling (TUNEL) staining was not increased when compared with control mice fed *ad libitum*, whereas TUNEL$^+$ cells were very rare and found only in luminal surface EC (Supplementary Fig. S1b). This indicated that mucosal thickness did not change significantly because of an appropriately balanced rate of cell turnover, that is, enhanced proliferation with increased shedding rate of EC. This transient hyperproliferation of colonic EC was observed in several mouse strains, irrespective of gender or age (Supplementary Fig. S2a–c). We also found that starvation for only 12 h was sufficient to evoke the same refeeding-induced hyperproliferation response (Supplementary Fig. S2d). Thus, even transient starvation has a substantial impact on colonic EC turnover. Because a 12-h starvation period would be expected to occur on a daily basis, we also examined the daily changes in colonic EC proliferation without a controlled starvation period. As expected, considerable fluctuation in the number of BrdU+ cells was observed (Supplementary Fig. S2e). A high number of proliferating cells, comparable to the increased proliferation observed in refed mice, was seen at approximately noon in our facility. This observation does fit with mice being more active and feeding during the dark cycle and falling asleep (and presumably fasting) during the light cycle.

Because significantly increased EC proliferation was seen in the colon but not in the small intestine, we hypothesized that microbiota may be involved in the underlying mechanisms. Presence of microbiota stimulates innate immune responses through bacterial components, as well as fermentation products. To test the importance of the microbiota for EC proliferation responses to starvation-refeeding, mice were given oral antibiotics. Hyperproliferation in the colon was not observed in mice treated with antibiotics, although recovery of the small intestine was unaffected (Fig. 2a). As fermentation of dietary fibre depends on the action of microbiota, we also eliminated fibre from the mouse diet using a powdered formula of oral rehydration solution (ORS) containing glucose and salt, or an elemental diet containing dextran with amino acids and other nutritional supplements for refeeding after starvation. The small intestinal cell turnover in treated mice was similar to mice fed with normal bait (CE2). However, hyperproliferation in the colon did not take place in the absence of dietary fibre (Fig. 2a). The importance of microbiota in refeeding-induced colonic hyperproliferation was further confirmed in germ-free mice. In these mice, starvation-refeeding induced the transient decrease in BrdU$^+$ cells with subsequent recovery in the small intestine similar to that observed in specific pathogen-free (SPF) mice. However, the refeeding-induced colonic hyperproliferation was not observed in germ-free mice (Fig. 2b), consistent with the results obtained from SPF mice treated with antibiotics. From these results, we conclude that accelerated colonic EC turnover after starvation-refeeding is triggered by a microbiota-dependent mechanism. Lack of hyperproliferation in ORS or elemental diet refed mice suggests that degradation products of dietary fibre by live bacteria are required to support the hyperproliferation response.

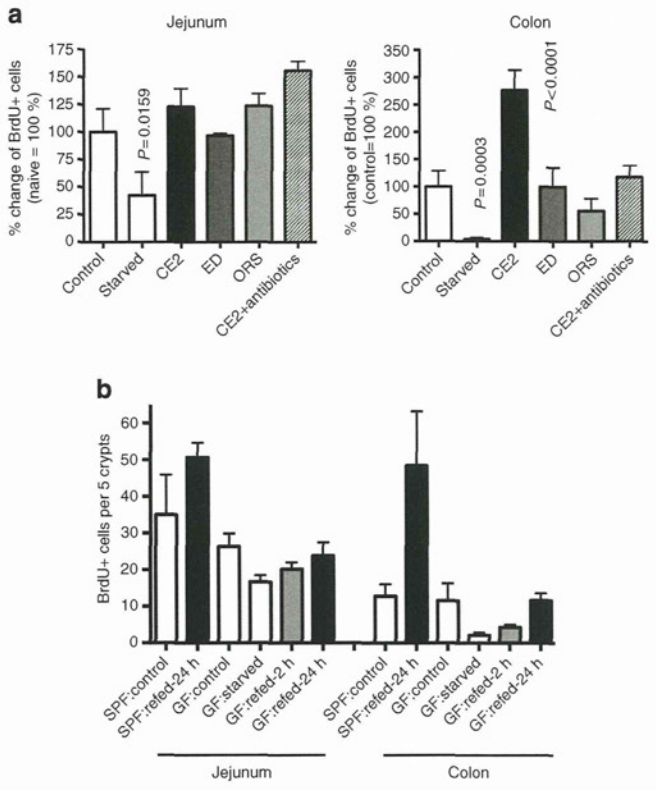

Figure 2 | Requirement for live microbiota and dietary fibre for refed-induced hyperproliferation. (**a**) Mice were starved for 36 h and refed with CE2, ED or ORS. A group of mice refed with CE2 was also given oral antibiotics. The percentage of BrdU+ cells per crypt in the colon 12 h after refeeding was compared (control = 100%). Data are shown as an average + s.d. for 4–6 mice for each group. Statistically significant differences from the control group are indicated with a *P*-value (Mann-Whitney test). (**b**) Germ-free mice were starved for 36 h and refed CE2 for the indicated time. Data are shown as an average + s.d. for three mice for each group.

***Lactobacillus murinus* induced accelerated EC turnover.** The importance of microbiota in refeeding-induced colonic hyperproliferation prompted us to investigate possible alterations in the composition of microbiota during starvation and refeeding. The number of bacteria decreased in both the small and large intestines after starvation. Bacterial numbers recovered to ~50% of baseline at 24 h in the small intestine of mice refed either CE2 or ORS. In contrast, the number of bacteria was approximately twofold greater in the colons of refed animals than in the colons of untreated controls (Fig. 3a). Thus, bacterial outgrowth occurred in the refed-phase concomitant with hyperproliferation in the colon. In fluorescence *in situ* hybridization (FISH) using a universal probe for the bacterial 16S rRNA sequence, overgrown bacteria adhered onto the surfaces of the EC, even in the deep pits of the crypts, which was not observed in control mice (Fig. 3b). However, bacterial translocation across the EC layer was not observed using FISH. The composition of the microbiota analyzed by denaturing gradient gel electrophoresis (DGGE) demonstrated that *Lactobacillus murinus* was a major species in the small intestines of control mice, which disappeared after starvation (Supplementary Fig. S3). The bacterium related to *Streptococcus alactolyticus* was detected in the small intestines of animals starved or refed for 2 h, and *L. murinus* reappeared in either CE2- or ORS-refed mice. In the colon, appearance of *L. murinus* was detected only in CE2-refed mice but not in control, starved or ORS-refed mice (Fig. 3c). Further, starvation-refeeding experiments using gnotobiotic mice monoassociated with *L. murinus* showed that presence of *L. murinus* alone was able to reconstitute colonic EC hyperproliferation in refed mice (Fig. 3d,e). Thus, colonic EC hyperproliferation on refeeding seems tightly associated with the outgrowth of *L. murinus*.

Lactate and *L. murinus*-induced EC hyperproliferation. To identify the inducer of colonic EC hyperproliferation, we

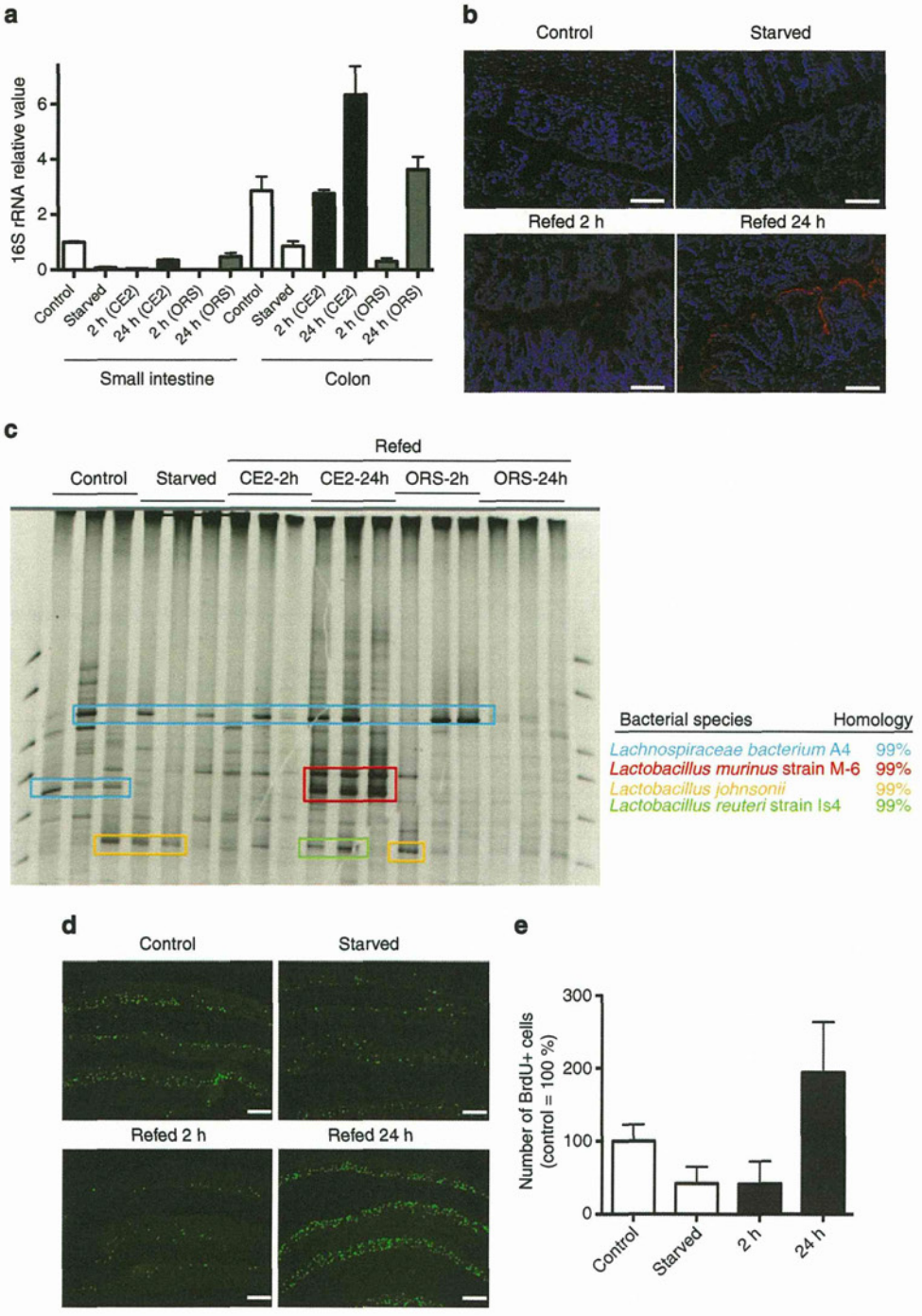

Figure 3 | Colonic EC hyperproliferation is induced by *Lactobacillus murinus*. (**a**) Number of bacteria determined by the 16S rRNA value. Mice were starved for 36 h and refed with the indicated formula in parentheses for the indicated time duration. Data are shown as an average + s.d. for three mice for each group. (**b**) FISH analysis of the starvation-refed colon with the 16S RNA probe. Scale bar, 100 μm. (**c**) DGGE analysis of colonic luminal contents in control mice and mice starved for 36 h and refed with CE2 or ORS for 2 or 24 h. Colonic luminal contents were collected and the microbial species determined, as described in the Methods. Each lane represents samples from individual mice. (**d**) Gnotobiotic mice were generated by inoculation of *Lactobacillus murinus* into germ-free mice. Frozen sections were stained by anti-BrdU antibody (green). Scale bar, 200 μm. (**e**) Number of BrdU + cells is shown as relative to control gnotobiotic mice. Data are shown as an average + s.d. for three mice for each group.

attempted to reconstitute hyperproliferation in ORS-refed mice. As shown in Fig. 4a, we first confirmed that intrarectal injection of fresh caecal contents from starvation-CE2-refed mice into ORS-refed mice fully induced hyperproliferation, demonstrating that intestinal luminal contents are critical for the hyperproliferation response. Rectal administration of ultraviolet-killed total flora or *L. murinus* (1×10^{10} colony-forming units, 0.1 ml per mouse) only partially reconstituted CE2-refed hyperproliferation, suggesting that live bacterial metabolites may be required for the full response. To identify the hyperproliferation-inducing factor(s), metabolome analysis of the colonic luminal contents was performed using a gas chromatography–mass spectrometry (GC–

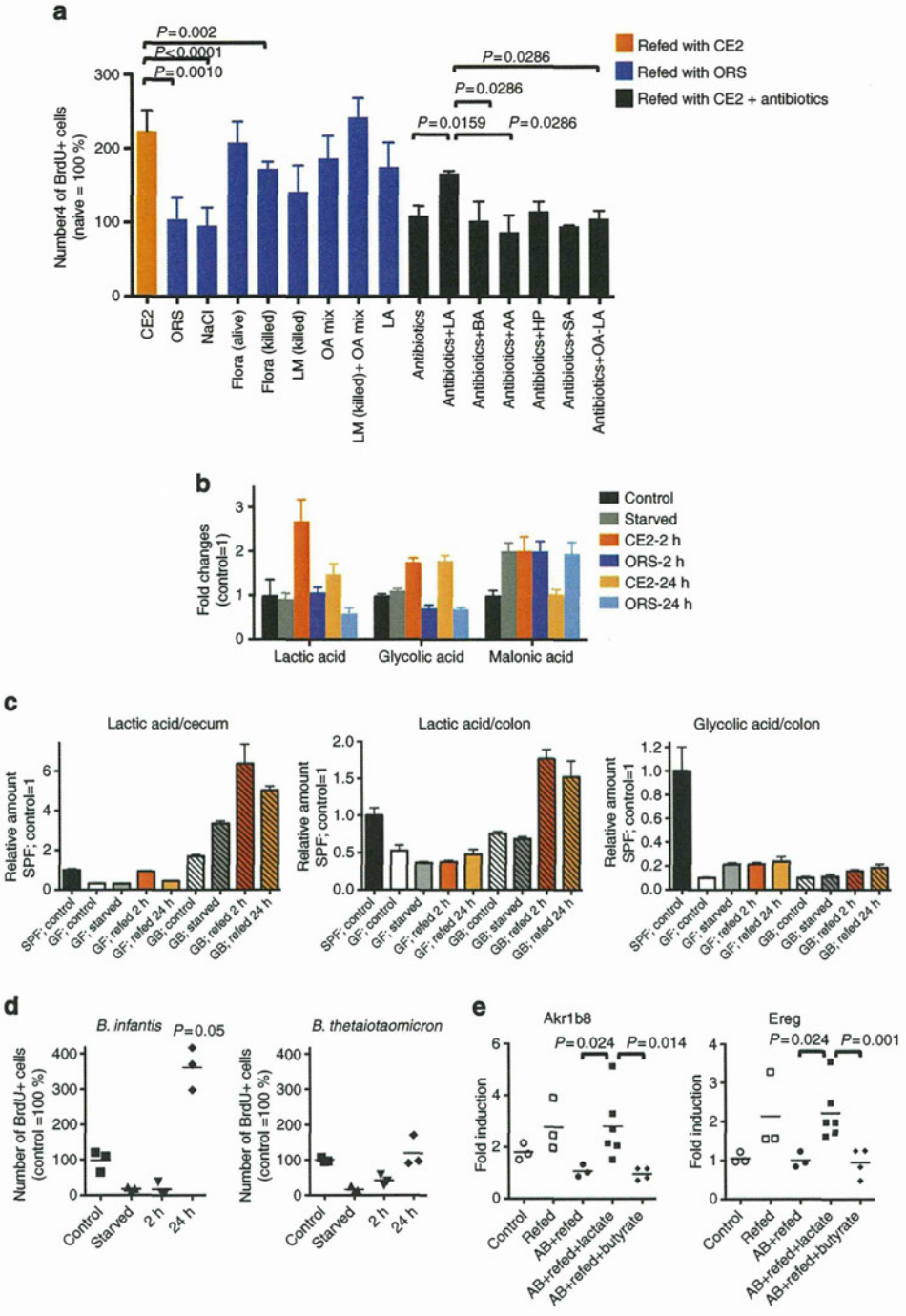

Figure 4 | Lactate is required for hyperproliferation. (**a**) Mice were starved for 36 h and refed CE2 (orange) or ORS (blue) or CE2 with oral antibiotics (black) for 12 h. In ORS-refed mice, the number of BrdU+ cells in the colon without rectal injection (ORS), with rectal injection of control 500 mM NaCl (NaCl), fresh caecal contents from CE2-refed mice (flora-alive), killed flora (flora-killed), killed *L. murinus* (LM-killed), organic acid mixture (OA mix), LM-killed plus organic acid mixture (LM-killed + OA mix), 500 mM lactate (LA) or a combination of these are shown. In mice refed with CE2 and treated with oral antibiotics, 500 mM NaCl (antibiotics), lactate (LA), butyrate (BA), acetate (AA), 3-hydroxypropionate (HP), succinate (SA) or OA mixture minus lactate (OA − LA) was administered intrarectally together with antibiotics three times during refeeding. Data are shown as the average + s.d. of 3–7 mice relative to control (fed *ad libitum*) mice. (**b**) Typical patterns of metabolome analysis as relative changes from the control condition. Data are shown as the average + s.d. of three mice as the relative signal intensity to control SPF mice. (**c**) Relative amount of lactic acid in the caecum and colon, and glycolic acid in the colon from starvation-refed, germ-free (GF) and gnotobiotic mice monoassociated with *L. murinus* (GB, hatched). Data are shown as the mean + s.d. of three mice as the relative signal intensity to control SPF mice. (**d**) Number of BrdU+ cells in the colon of gnotobiotic mice monoassociated with lactate-producing *Bifidobacterim infantis* or non-lactate-producing *Bacteroides thetaiotaomicron* shown as % of control (fed *ad libitum*). Short bar indicates the mean value. (**e**) Gene expression in the colon. Mice were starved for 36 h and refed CE2. Some mice were treated with oral antibiotics (AB), and 500 mM lactate or butyrate was administered intrarectally together with antibiotics three times during refeeding. After 12 h of refeeding, distal 1/3 of the colon was subjected to total RNA extraction and quantitative RT-PCR for Akr1b8 and Ereg. Data were shown as relative expression (AB + refed = 1). Each dot represents individual mice, and short bar indicates the mean value. In panels **a**, **d** and **e**, *P*-values were calculated using Mann–Whitney test.

MS) system (Supplementary Fig. S4). Some amino acids were markedly decreased in starved mice and recovered to control levels on refeeding with either CE2 or ORS, except aspartic acid, asparagines and glutamine, which did not return to control levels in ORS-refed mice. We found that organic acids were classified into at least two groups according to the pattern of alteration during starvation-refeeding. One group increased in CE2-refed mice but not in ORS-refed mice, which included lactic acids, glycolic acid, 3-hydroxypropanoic acid, maleic acid, glutaric acid, 2-deoxytetronic acid, 3-hydroxyphenylacetic acid and 4-hydroxybenzoic acid. The second group increased in starved mice and decreased after CE2-refeeding but not after ORS-refeeding, and included caproic acid, 2-hydroxybutyric acid, 2-hydroxyisovaleric acid, 4-hydroxyphenylacetic acid and malonic acid. Representative organic acids of these two groups are shown in Fig. 4b. Most fatty acids analyzed and urea showed similar kinetic patterns to the second group of organic acids (Supplementary Fig. S4). As we found that live *Lactobacillus* and its metabolite(s) were required for colonic EC hyperproliferation, we hypothesized that organic acids that increased on refeeding (that is, the first group) were most likely associated with EC hyperproliferation. On the basis of the total ion peak values of the GC–MS analysis (Supplementary Fig. S5a) and a separate analysis of luminal contents using NMR from control mice (Supplementary Fig. S5b), the composition of organic acid was estimated. According to these results, a mixture containing acetic acid, propionic acid, butyric acid, lactic acid, 3-hydroxypropionic acid, glycolic acid, succinic acid and glyceric acid was tested for its ability to support EC hyperproliferation on refeeding. This mixture induced hyperproliferation (that is, increased the number of $BrdU^+$ cells) more efficiently than ultraviolet-killed *L. murinus*, and co-administration of this mixture with killed bacteria induced the full hyperproliferative response (Fig. 4a). As *L. murinus* produces mainly lactate, we treated ORS-refed animals with 500 mM lactate alone rectally and examined colonic EC proliferation. Lactate alone resulted in EC hyperproliferation comparable to that of the organic acid mixture, indicating that this component was largely responsible for the observed response. To further confirm the action of lactic acid, mice refed with CE2 were treated orally and rectally with antibiotics and either lactate, butyrate, acetate, 3-hydroxypropanoate and succinate. As shown in Fig. 4a, only lactate induced EC hyperproliferation on refeeding, and deletion of lactate from the organic acid mixture resulted in the loss of hyperproliferation. This indicated that lactate was the most important organic acid for stimulation of colonic EC turnover in response to starvation-refeeding. Indeed, in germ-free mice, there were no significant changes in the amount of lactic acid during starvation-refeeding, while increased lactic acid was evident in the cecums and colons of *L. murinus*-monoassociated mice on refeeding (Fig. 4c). Glycolic acid, which also increased in the refed colons of SPF mice (Fig. 4b), did not change significantly on starvation-refeeding in germ-free mice and there were no differences in the levels of glycolic acid between germ-free and *L. murinus*-monoassociated mice. In summary, outgrowth of *L. murinus* and, therefore, production of lactic acid, induced the hyperproliferation of colonic EC. To further confirm this finding, we prepared gnotobiotic mice monoassociated with lactate-producing *Bifidobacterim longum* subsp. *infantis* (*B. infantis*) and non-lactate-producing *Bacteroides thetaiotaomicron* (*B. thetaiotaomicron*)[17,18]. As shown in Fig. 4d, starvation-refed *B. infantis*-monoassociated mice demonstrated hyperproliferation at refeeding. On the other hand, *B. thetaiotaomicron* did not induce hyperproliferation. These results clearly demonstrate that a bacterial metabolite (lactate) rather than bacterial components has a major role to induce accelerated cell turnover.

Upregulation of energy production pathway in refed colon EC. To characterize the signature of hyperproliferative EC induced by refeeding, we compared the gene expression profiles of purified EC derived from refed mice and refed mice treated with antibiotics. Pathway analysis showed that genes increased 1.5-fold in refed EC than in refed EC treated with antibiotics indicated the enrichment of the genes related to energy production, lipid metabolism, small-molecule biochemistry as the top networks, and glycerolipid metabolism as the top canonical pathway as shown in Tables 1 and 2 and in Supplementary Figs S6 and S7. This finding indicates that refed EC actively produce energy using stored fat. The glycerolipid metabolism pathway shown in Supplementary Fig. S7 clearly indicated increased fatty acid release from glycerolipids. The fatty acids that underwent beta-oxidation into acetyl CoA can eventually enter the tricarboxylic acid cycle to produce ATP, suggesting that the presence of luminal lactate facilitates ATP production through enhanced use of lipids.

To confirm that this gene expression profile is related to lactate in the lumen, we attempted to validate the result with quantitative PCR with reverse transcription (RT–PCR) using fresh colon exposed to lactate. *Akr1b8*, encoding aldo-keto reductase family 1, member B8, listed as enzyme commission number 1.1.1.21 in Supplementary Fig. S7, was one of top 10 genes enriched in refed colon (Supplementary Fig. S8). *Ereg* encodes epiregulin, a member of epidermal growth factor family and 1.7-fold higher in refed colon than that treated with antibiotics (Supplementary Fig. S8). As shown in Fig. 4e, both gene levels tended to be higher in refed mice than those of mice fed *ad libitum* (control). This upregulation was not seen in refed mice treated with antibiotics; However, additional rectal injection of lactate significantly upregulated both genes. Butyrate failed to induce expression of these genes in

Table 1 | Top five gene networks of 1.5-fold upregulated genes in colonic EC from refed mice compared with refed mice treated with antibiotics.

Associated network functions	Score
Energy production, lipid metabolism, small-molecule biochemistry	50
Cell death, reproductive system development and function, haematological disease	39
Post-translational modification, carbohydrate metabolism, lipid metabolism	29
Lipid metabolism, small-molecule biochemistry, vitamin and mineral metabolism	27
Lipid metabolism, small-molecule biochemistry, molecular transport	26

Table 2 | Top five canonical pathways of 1.5-fold upregulated genes in colonic EC from refed mice compared with refed mice treated with antibiotics.

Top canonical pathways	*P*-value*
Glycerolipid metabolism	1.04E-06
Metabolism of xenobiotics by cytochrome P450	2.23E-05
Linoleic acid metabolism	2.46E-05
LPS/IL-1-mediated inhibition of RXR function	3.33E-05
Arachidonic acid metabolism	3.24E-04

*The generated canonical pathways were ranked by *P*-values, which were calculated using a Fisher's exact test by comparing the number of the selected genes relative to the total number of occurrences of these genes in all functional/pathway annotations stored in the Ingenuity Pathways Knowledge Base.

antibiotic-treated mice. These results further support the notion that lactate changes the gene expression of EC and drives metabolic shift to enhance cell proliferation in refed mice.

Starvation-refeeding alters susceptibility to carcinogen. Our observation that colonic EC turnover is accelerated after starvation-refeeding in the presence of microbiota prompted us to test whether this proliferative response to refeeding sensitizes colonic EC to tumorigenesis. To this end, we employed a mouse model of tumorigenesis using the chemical carcinogen azoxymethane (AOM), which induces aberrant crypt foci (ACF) of the colon. The experimental protocol is illustrated in Supplementary Fig. S9. In mice given AOM 8 h after the initiation of refeeding, at the beginning of hyperproliferation of the colon, the number of ACF was significantly higher than in mice fed *ad libitum* (Fig. 5a). In contrast, when mice were challenged with AOM followed by starvation and refeeding, it resulted in a striking decrease in the number of ACF (Fig. 5a). In addition to ACF, the colonic mucosa of refed-plus AOM mice appeared rough and scraggly (Fig. 5b), matching the histological image, in which the deformed and atypical shapes of the crypts were scattered (Fig. 5c); however, crypts of mice with AOM followed by starvation had a smooth appearance (Fig. 5b) lined with goblet cells (Fig. 5c). As we thought that hyperproliferation was responsible for the increased number of ACF in refed-plus AOM mice, oral antibiotics were administered to AOM-treated mice during refeeding to block the production of lactic acid by *L. murinus* and thereby prevent EC hyperproliferation. This treatment reduced the number of ACF to that of control mice and decreased the irregularities observed in the colonic mucosa (Fig. 5a,c). These observations suggest that hyperproliferation in response to refeeding increases the number of AOM-susceptible cells, resulting in a greater number of ACF. In contrast, accelerated cell turnover after temporal starvation appears to eliminate damaged cells efficiently. Although AOM metabolism may drastically change during starvation and refeeding, expression levels of CYP2E1, a major enzyme associated with the activation of AOM, did not correlate with the number of ACF (Supplementary Fig. S9b). We think the metabolic rate of AOM is not a major factor that distinguishes sensitivity to DNA damage between starved and refed mice (Supplementary Discussion).

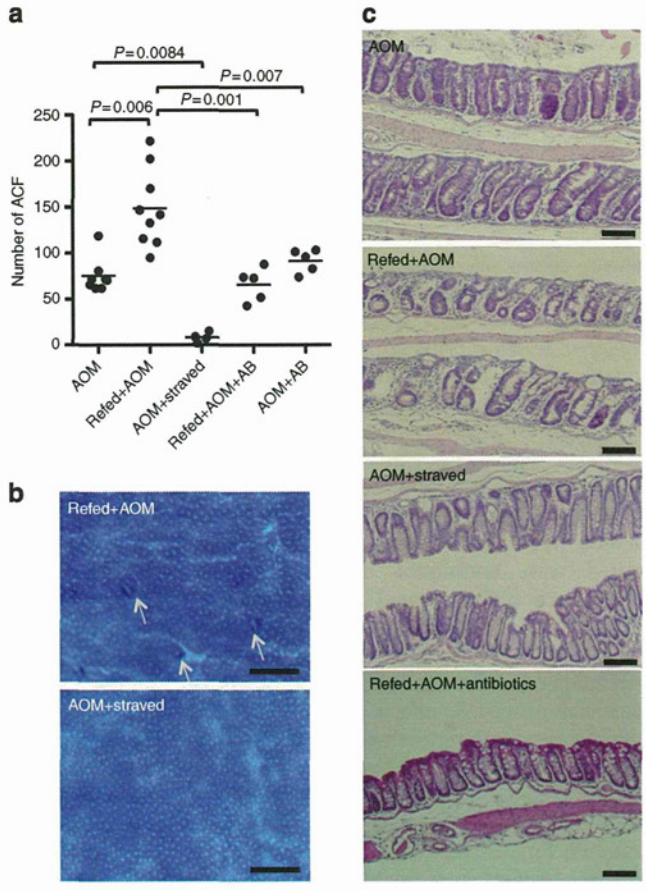

Figure 5 | Effects of starvation-refeeding on exposure to carcinogen. (**a**) The number of ACF in the colon. AOM, mice fed *ad libitum* and treated with AOM; Refed + AOM, treatment with AOM at refeeding; AOM + starved, mice fed *ad libitum* and treated with AOM, then starvation was begun on the following day; Refed + AOM + AB, refed + AOM mice were treated with oral antibiotics; AOM + AB, mice were fed *ad libitum* and treated with AOM and oral antibiotics. These treatments were repeated five times a week. A week after the last injection of AOM, ACF in the colon were quantified. Each dot indicates an individual mouse. *P*-values were calculated using Mann–Whitney test. For a detailed protocol, see Supplementary Fig. S9. (**b**) Methylene blue staining of the colon from Refed + AOM or AOM + starved mouse groups. Arrows indicate ACF. Images were captured with a stereomicroscope. Scale bar, 0.5 mm. (**c**) Formalin-fixed paraffin-embedded sections were stained with H&E. Scale bar, 100 μm. All images were taken from the same region of the colon (distal one-third).

Discussion

In this study, we found that transient starvation enhanced EC turnover on refeeding, and this response was dependent on the presence of commensal lactobacilli and its metabolite, lactate. We also found that carcinogen sensitivity was significantly increased during refeeding and was reduced by starvation after exposure to the carcinogen.

There are a limited number of studies on colonic EC turnover during starvation. Using the metaphase-arrest technique, it has been reported that there is reduced 'crypt cell production' during starvation and an 'overshooting' recovery after refeeding[2]; in rats, colonic EC responses are dependent on the presence of fermentable fibre[19]. Taken together with our results, these data indicate that our observations are not particular to our animal facility or animals colonized with certain microbiota. In this study, we identified lactic acid-producing *L. murinus* as the causal factor for the refeeding EC hyperproliferation response. As discussed below, because lactate was sufficient to accelerate EC turnover, many lactic acid-producing bacteria have the potential to induce a similar effect.

In our study, *L. murinus* was detected in control (fed *ad libitum*) conditions in the small intestine but was not a dominant strain in the colon at steady state. In some individual control mice, *L. murinus* was a major strain in the small intestine. In contrast, outgrowth of *L. murinus* was universally observed in the colons of refed mice. When the results of Fig. 3a–c are considered, *L. murinus* appeared to be the major constituent of refed colonic microbiota, apparently heavily attached to the mucosal surface. While *L. murinus* did reside in the small intestine before starvation, its outgrowth in the colon on starvation-refeeding was likely due to the luminal environment becoming particularly suitable for its growth. Colonization of *L. murinus* may be affected by changes in available nutrients, oxygen concentration, or host and microbial factors for adhesion, such as production and carbohydrate structure of host mucins, secretion of host antibacterial peptides and upregulation of microbial adhesins, including mucus-binding protein[20]. Indeed, luminal nutrients changed dramatically during starvation, and loss of villi in the small intestine reduced the available surface area for

bacterial adhesion. All these changes may have favored the growth of *L. murinus* in the refed colon. Refeeding with ORS provides glucose as the energy source, which may not reach the colon lumen, sustains morphological recovery of small intestine EC. However, ORS-refeeding failed to support *L. murinus* colonization or hyperproliferation of colonic EC. In the experiment using gnotobiotic mice, we showed that monoassociation with *L. murinus* was sufficient to induce colonic EC hyperproliferation in refed mice. Therefore, we conclude that outgrowth of *L. murinus* induced colonic EC hyperproliferation on refeeding.

In subsequent experiments, we identified lactate as the most important *L. murinus* metabolite for the induction of colon hyperproliferation. This conclusion is based on several pieces of evidence. First, metabolome analyses indicated that lactic acid levels increased substantially in the colons of CE2-refed animals but not in ORS-refed colons. Second, gnotobiotic mice monoassociated with *L. murinus* had contained elevated lactic acid levels in the colon, and gnotobiotic mice monoassociated with a lactate-producing stain but not a non-lactate-producing strain showed hyperproliferation after starvation. Third, in animals treated with antibiotics to eliminate normal flora, rectal administration of lactic acid but not butyrate or acetate supported colonic EC proliferation. This result surprised us, because butyrate and acetate are also major fermentation products of microbiota, and there is a wide range of evidence supporting their beneficial protective effects on colonic EC[21–25]. On the other hand, lactate has long been considered a dead-end waste product; however, some recent studies have shown that lactate has diverse metabolic and regulatory properties, such as being an energy source, a modulator of energy production, and a signalling molecule for cell repair and angiogenesis (reviewed in ref. 26). Further, survival and function of some types of cells such as neurons and germ cells that demand high energy depend on the extracellular lactate provided by adjacent nursing cells, astrocytes and Sertoli cells[27]. Although we did not obtain direct evidence that lactate itself is used as an energy source, we speculate that the modified redox status of EC by starvation-refeeding might enable EC to respond to luminal lactate to promote energy production.

On the basis of these observations, we posed the question, 'What is the significance of colonic hyperproliferation on refeeding to health and disease?' Treatment of refed animals with AOM clearly demonstrated that exposure to a carcinogen during the colonic hyperproliferation response to refeeding significantly increased the risk of tumorigenesis. In contrast, colonic hyperproliferation induced after exposure to a carcinogen appears to eliminate damaged cells efficiently. In general, starvation or calorie restriction has been reported to extend the lifespan of most species, including rodents and primates. The molecular basis for this observation has been proposed to be sirtuins and the nutritional signalling target of rapamycin pathway[28,29]. Studies also have shown that calorie restriction decreases the risk of colon cancer[30]; however, our study suggests that the timing of carcinogen exposure is a critical factor. After transient starvation, there is a window of time when colonic EC become susceptible to DNA damage, and this greatly depends on the bacterial flora and luminal metabolite composition. Thus, our results provide new insight into the relationship between carcinogenesis, food intake and lifestyle.

Methods

Mice. Six-week-old male BALB/c mice were used for all experiments, unless otherwise indicated. All mice were obtained from CLEA Japan Inc. (Tokyo, Japan), maintained under SPF conditions at the National Center for Global Health and Medicine facility (Tokyo, Japan), and fed normal bait (CE2, Clea Japan). Germ-free mice (BALB/c background) were purchased from Sankyo Labo Service Corporation, Inc. and kept in an animal facility in RIKEN. All experiments were performed according to the Institutional Guidelines for the Care and Use of Laboratory Animals in Research and the approval of the local ethics committee at the National Center for Global Health and Medicine and RIKEN.

Starvation and refeeding. During starvation, mice were kept in plastic cages with bedding chips and drinking water without bait. Irrespective of the length of the starvation period, the refeeding period was set to begin at 8:00 in all experiments. Elementary diet (Elental) was obtained from Ajinomoto Co. Inc.. Powdered formula of ORS contained 675 g glucose, 130 g NaCl, 145 g trisodium citrate dihydrate and 75 g KCl mixed in a sterilized mortar. To eliminate endogenous flora, a 0.2-ml solution of 500 mg l^{-1} metronidazol and 1 g l^{-1} vancomycin was administered daily by oral–gastric gavage. After starvation, 12- and 24-h refeeding with elemental diet or ORS were able to recover body weights comparable to CE2.

In enema experiments, ultraviolet irradiation-killed *L. murinus* was prepared, and pelleted cells were re-suspended in PBS (1×10^{10} colony-forming units; 0.1 ml per mouse). For intrarectal administration of the reagents, 0.1 ml of the indicated solution was injected into the rectum three times within the first 12 h of refeeding (0, 4 and 8 h after refeeding), and animals were lightly anesthetized using inhaled sevoflurane. The organic acid mixture contained 600 mM acetic acid, 200 mM propionic acid, 200 mM butyric acid, 200 mM lactic acid, 200 mM 3-hydroxypropionic acid, 100 mM glycolic acid, 40 mM succinic acid and 200 mM glyceric acid (final concentrations). In some experiments, antibiotics (50 mg l^{-1} metronidazol and 0.1 g l^{-1} vancomycin, final concentration) were added to the solutions for rectal injection.

Microbiological analysis

16S rRNA. Bacterial genomic DNA was isolated as described previously with some modifications[31]. In brief, faecal samples were freeze-dried, homogenized, disrupted using 0.1-mm Zirconia/Silica Beads, and extracted with 10% sodium dodecyl sulphate/Tris-HCl plus ethylenediamine tetraacetic acid (EDTA) buffer solutions. Bacterial genomic DNA was purified from the faecal extracts using a phenol/chloroform/isoamyl alcohol method. Bacterial genomic DNA samples were amplified using SYBR premix Ex Taq (TAKARA BIO, Otsu, Japan) and universal primers for the genes encoding bacterial 16S rRNA[22,32]. The results were calculated as the amount relative to copy number detected in the small intestinal contents of control mice.

DGGE analysis. Bacterial genomic DNA samples were amplified by PCR with universal bacterial primers 954f and 1396r specific for the V6 to V8 regions of the 16S rRNA gene[33]. The reaction mixtures and PCR conditions were described previously[32]. After confirmation of the PCR product by agarose gel electrophoresis, DGGE was performed with the DCode universal mutation detection system (Bio-Rad Lab., Irvine, CA). Polyacrylamide gel conditions for the denaturing gradient, migration, and differentiation were described previously[33]. Electrophoresis was conducted with a constant voltage of 82 V at 60 °C for 15 h. Gels were stained with SYBR Green I (Lonza, Rockland, ME) and acquired by GelDoc XR (Bio-Rad Lab)[31].

Fluorescence in situ hybridization. Bacterial 16s rRNA FISH was performed as described previously[34]. In brief, colonic tissue sections were fixed in 4% paraformaldehyde, washed in PBS, incubated in 50 µl of 30% formamide hybridization buffer containing 25 ng of 5′-Cy3-labelled universal oligonucleotide probes for eubacteria (EUB338, 5′-GCTGCCTCCCGTAGGAGT-3′) or the non-bacterial control (NONEUB, 5′-ACTCCTACGGGAGGCAGC-3′) for 90 min at 46 °C, and washed with the same stringency for 20 min at 48 °C. Stained sections were imaged on a DM-IRE2 confocal laser-scanning microscope (Leica Microsystem).

Metabolome-GC/MS analysis and data processing. Intestinal contents were collected and lyophilized. To extract low-molecular-weight metabolites, 10 mg of lyophilized intestinal contents were transferred to a clean tube and homogenized in 1,000 µl solvent mixture ($MeOH:H_2O:CHCl_3 = 2.5:1:1$). Then, 10 µl of 0.5 mg ml^{-1} 2-isopropylmalic acid (Sigma-Aldrich, Tokyo, Japan) dissolved in distilled water was added to each tube, and the mixture was mixed well. The mixture was shaken at 1,200 r.p.m. for 30 min at 37 °C before being centrifuged at 16,000*g* for 3 min at 4 °C. Nine-hundred microliters of the resultant supernatant were collected into a clean tube. Four-hundred fifty microliters of $CHCl_3$ were added to the collected supernatant and centrifuged at 16,000*g* for 3 min at 4 °C, and 500 µl of supernatant were collected in a clean tube. Two-hundred microliters of distilled water were added to the collected supernatant and centrifuged at 16,000*g* for 3 min at 4 °C; 500 µl of supernatant were collected in a clean tube. The collected supernatant was lyophilized using a freeze-dryer before oximation and the following derivatization. For oximation, 80 µl of 20 mg ml^{-1} methoxyamine hydrochloride (Sigma-Aldrich), dissolved in pyridine, was mixed with a lyophilized sample before being shaken at 1,200 r.p.m. for 90 min at 30 °C. Next, 40 µl *N*-methyl-*N*-trimethylsilyl-trifluoroacetamide (GL Science, Tokyo, Japan) were added for derivatization, and the mixture was incubated at 1,200 r.p.m. for 30 min

at 37 °C. The mixture was centrifuged at 16,000*g* for 5 min at 4 °C, and the resultant supernatant was subjected to GC–MS analysis.

According to our previous reports[35,36], GC–MS analysis was performed using GCMS-QP2010 Plus (Shimadzu Co., Kyoto, Japan) with a DB-5 column (30 m × 0.25 mm inner diameter; film thickness is 1.00 μm, J&W Scientific, Folsom, CA) and GCMS-QP2010 Ultra (Shimadzu Co., Kyoto, Japan) with a CP-SIL 8 CB low-bleed/MS column (30 m × 0.25 mm inner diameter, film thickness is 0.25 μm, Agilent Co., Palo Alto, CA). Processing of data obtained from GCMS-QP2010 Plus and GCMS-QP2010 Ultra was carried out as described previously[35,36]. For semi-quantification, the peak heights of each ion were calculated and normalized using the peak height of 2-isopropylmalic acid as an internal standard.

Metabolome-NMR analysis. NMR-based metabolomics was performed as described previously with minor modifications[37]. In brief, faecal metabolites from mice were extracted by gentle shaking with 100 mM potassium phosphate buffer containing 90% deuterium oxide and 1 mM sodium 2,2-dimethyl-2- silapentane-5-sulfonate as the chemical shift references ($\delta = 0.0$ p.p.m.), and analyzed by ^{1}H-NMR and ^{1}H, ^{13}C-NMR. Metabolite annotations were performed using our standard database[38].

Induction of ACF. As shown in Supplementary Fig. S9, mice were divided into five groups. Group 1 (AOM) was fed *ad libitum* and intraperitoneally injected with AOM (Sigma-Aldrich, 10 mg kg^{-1}). Group 2 (refed + AOM) was starved for 24 h, refed with CE2 and injected with AOM 8 h after refeeding. Group 3 (AOM + starved) was injected with AOM at 16:00; fasting for 24 h was begun at 8:00 on the following day. Group 4 (refed + AOM + AB) was treated similar to Group 2 but oral antibiotics were administered, as described above, beginning with a 5-day starvation period. Group 5 (AOM + AB) was fed *ad libitum*, injected with AOM and given oral antibiotics for 5 days. These protocols were repeated weekly, five times. All mice groups were given AOM injections at 16:00. On day 37, colon tissues were obtained, washed and extended by flushing with PBS. Colons were opened longitudinally, fixed with formalin and stained with 3% methylene blue. ACF were enumerated under a stereomicroscope[39].

Gene expression profiling of colon ECs. For global gene expression profiling in EC, colon tissues were stirred in 6.5 mM dithiothreitol in Hank's Balanced Salt Solution for 15 min at room temperature and in 10 mM EDTA in Hank's Balanced Salt Solution for 10 min. Treatment with EDTA was repeated 4–6 times until EC were released from the stroma. Single-cell suspensions of EC were stained with 7-amino-actinomycin D, fluorescein isothiocyanate-anti-CD45 and phycoerythrin-anti-EpCAM antibodies (BD). Viable EpCAM^{+}CD45^{-} cells were sorted as purified EC (Moflo, Beckman Coulter, Tokyo, Japan). Total RNA was extracted according to standard protocols (Affymetrix). Targets were prepared and hybridized to the GeneChip Mouse Gene 1.0 ST Array (Affymetrix) according to standard protocols. GeneChip data sets were analyzed using GeneSpring GX 11 (Agilent). Array data were normalized using robust multi-array analysis algorithms.

Statistical analysis. All data are presented as the mean ± s.d., unless indicated in the legend. For comparison of two groups, a non-parametric method (Mann–Whitney test) and Student's *t*-test were used in comparisons as indicated in the legends. Results were determined as significant when *P*-values were less than 0.05. Statistical analyses were performed using GraphPad Prism 4 software (GraphPad Software, Inc).

Methods for histological analyses, quantitative RT–PCR, and pathway analysis of gene expression profiling are described in the Supplementary Information.

References

1. Heath, J. P. Epithelial cell migration in the intestine. *Cell Biol. Int.* **20,** 139–146 (1996).
2. Goodlad, R. A. & Wright, N. A. The effects of starvation and refeeding on intestinal cell proliferation in the mouse. *Virchows Arch. B Cell Pathol. Incl. Mol. Pathol.* **45,** 63–73 (1984).
3. Scheving, L. E., Tsai, T. H. & Scheving, L. A. Chronobiology of the intestinal tract of the mouse. *Am. J. Anat.* **168,** 433–465 (1983).
4. Buchi, K. N., Moore, J. G., Hrushesky, W. J., Sothern, R. B. & Rubin, N. H. Circadian rhythm of cellular proliferation in the human rectal mucosa. *Gastroenterology* **101,** 410–415 (1991).
5. Marra, G. *et al.* Circadian variations of epithelial cell proliferation in human rectal crypts. *Gastroenterology* **106,** 982–987 (1994).
6. Carey, H. V. Seasonal changes in mucosal structure and function in ground squirrel intestine. *Am. J. Physiol.* **259,** R385–R392 (1990).
7. Carey, H. V., Andrews, M. T. & Martin, S. L. Mammalian hibernation: cellular and molecular responses to depressed metabolism and low temperature. *Physiol. Rev.* **83,** 1153–1181 (2003).
8. Secor, S. M. & Diamond, J. A vertebrate model of extreme physiological regulation. *Nature* **395,** 659–662 (1998).
9. Hoogerwerf, W. A. *et al.* Clock gene expression in the murine gastrointestinal tract: endogenous rhythmicity and effects of a feeding regimen. *Gastroenterology* **133,** 1250–1260 (2007).
10. Steiner, M., Bourges, H. R., Freedman, L. S. & Gray, S. J. Effect of starvation on the tissue composition of the small intestine in the rat. *Am. J. Physiol.* **215,** 75–77 (1968).
11. Kudsk, K. A. Effect of route and type of nutrition on intestine-derived inflammatory responses. *Am. J. Surg.* **185,** 16–21 (2003).
12. Kudsk, K. A. *et al.* Enteral versus parenteral feeding. Effects on septic morbidity after blunt and penetrating abdominal trauma. *Ann. Surg.* **215,** 503–513 (1992).
13. Roberfroid, M. B., Bornet, F., Bouley, C. & Cummings, J. H. Colonic microflora: nutrition and health. Summary and conclusions of an International Life Sciences Institute (ILSI) [Europe] workshop held in Barcelona, Spain. *Nutr. Rev.* **53,** 127–130 (1995).
14. Arumugam, M. *et al.* Enterotypes of the human gut microbiome. *Nature* **473,** 174–180 (2011).
15. Wu, G. D. *et al.* Linking long-term dietary patterns with gut microbial enterotypes. *Science* **334,** 105–108 (2011).
16. Maslowski, K. M. & Mackay, C. R. Diet, gut microbiota and immune responses. *Nat. Immunol.* **12,** 5–9 (2011).
17. Macfarlane, S. & Macfarlane, G. T. Regulation of short-chain fatty acid production. *Proc. Nutr. Soc.* **62,** 67–72 (2003).
18. Sonnenburg, J. L., Chen, C. T. & Gordon, J. I. Genomic and metabolic studies of the impact of probiotics on a model gut symbiont and host. *PLoS Biol.* **4,** e413 (2006).
19. Goodlad, R. A. *et al.* Proliferative effects of 'fibre' on the intestinal epithelium: relationship to gastrin, enteroglucagon and PYY. *Gut* **28**(Suppl): 221–226 (1987).
20. Roos, S. & Jonsson, H. A high-molecular-mass cell-surface protein from Lactobacillus reuteri 1063 adheres to mucus components. *Microbiology* **148,** 433–442 (2002).
21. Donohoe, D. R. *et al.* The microbiome and butyrate regulate energy metabolism and autophagy in the mammalian colon. *Cell Metab.* **13,** 517–526 (2011).
22. Fukuda, S. *et al.* Bifidobacteria can protect from enteropathogenic infection through production of acetate. *Nature* **469,** 543–547 (2011).
23. Okamoto, T. *et al.* Preventive efficacy of butyrate enemas and oral administration of Clostridium butyricum M588 in dextran sodium sulfate-induced colitis in rats. *J. Gastroenterol.* **35,** 341–346 (2000).
24. Scheppach, W. Treatment of distal ulcerative colitis with short-chain fatty acid enemas. A placebo-controlled trial. German-Austrian SCFA Study Group. *Dig. Dis. Sci.* **41,** 2254–2259 (1996).
25. Scheppach, W. *et al.* Effect of butyrate enemas on the colonic mucosa in distal ulcerative colitis. *Gastroenterology* **103,** 51–56 (1992).
26. Sola-Penna, M. Metabolic regulation by lactate. *IUBMB Life* **60,** 605–608 (2008).
27. Gladden, L. B. Lactate metabolism: a new paradigm for the third millennium. *J. Physiol.* **558,** 5–30 (2004).
28. Bordone, L. & Guarente, L. Calorie restriction, SIRT1 and metabolism: understanding longevity. *Nat. Rev. Mol. Cell. Biol.* **6,** 298–305 (2005).
29. Colman, R. J. *et al.* Caloric restriction delays disease onset and mortality in rhesus monkeys. *Science* **325,** 201–204 (2009).
30. Omodei, D. & Fontana, L. Calorie restriction and prevention of age-associated chronic disease. *FEBS Lett.* **585,** 1537–1542 (2011).
31. Date, Y. *et al.* New monitoring approach for metabolic dynamics in microbial ecosystems using stable-isotope-labeling technologies. *J. Biosci. Bioeng.* **110,** 87–93 (2010).
32. Muyzer, G. *et al.* In *Molecular Microbial Ecology Manual* Vol. 3.4.4 (eds Akkermans, A., van Elsas, J. D. & de Bruijin, F., 1998).
33. Yu, Z. & Morrison, M. Comparisons of different hypervariable regions of rrs genes for use in fingerprinting of microbial communities by PCR-denaturing gradient gel electrophoresis. *Appl. Environ. Microbiol.* **70,** 4800–4806 (2004).
34. Nenci, A. *et al.* Epithelial NEMO links innate immunity to chronic intestinal inflammation. *Nature* **446,** 557–561 (2007).
35. Shiomi, Y. *et al.* GCMS-based metabolomic study in mice with colitis induced by dextran sulfate sodium. *Inflamm. Bowel Dis.* **17,** 2261–2274 (2011).
36. Tsugawa, H. *et al.* Practical non-targeted gas chromatography/mass spectrometry-based metabolomics platform for metabolic phenotype analysis. *J. Biosci. Bioeng.* **112,** 292–298 (2011).
37. Fukuda, S. *et al.* Evaluation and characterization of bacterial metabolic dynamics with a novel profiling technique, real-time metabolotyping. *PLoS One* **4,** e4893 (2009).
38. Nakanishi, Y. *et al.* Dynamic omics approach identifies nutrition-mediated microbial interactions. *J. Proteome Res.* **10,** 824–836 (2011).
39. Osawa, E. *et al.* Predominant T Helper Type 2-inflammatory responses promote murine colon cancers. *Int. J. Cancer* **118,** 2232–2236 (2006).

Acknowledgements

This work was supported partly by grants and contracts from the programme Grants-in-Aid for Scientific Research (B) and Grants-in-Aid for Young Scientists (B) from the Ministry of Education, Cultures, Sports, Science, and Technology; Japan Science and Technology Agency; a grant from the National Center for Global Health and Medicine (21-110, 22-205, 21-129), Ministry of Health, Labor, and Welfare; RIKEN RCAI; and Health and Labor Sciences Research Grants for research on intractable diseases from Ministry of Health, Labor and Welfare of Japan; grants for the Global COE Program, Global Center of Excellence for Education and Research on Signal Transduction Medicine in the Coming Generation from the Ministry of Education, Culture, Sports, Science, and Technology of Japan (M. Yoshida); and for the project research (Development of fundamental technology for analysis and evaluation of functional agricultural products and functional foods) from the Ministry of Agriculture, Forestry, and Fisheries of Japan (M. Yoshida). We thank Dr M. Tamura-Nakano in NCGM EM Support Unit for her technical support for histological analysis.

Author contributions

T. D. designed the study, analyzed data and wrote the paper. T. Okada developed the experimental system, performed *in vivo* experiments and analyzed data. S.F., K. Hase and H.O. performed experiments and analyzed data of germ-free and gnotobiotic mice, bacteriological analysis and gene profiling and wrote the paper. S.N, Y.I. and M. Yoshida performed chemical analyses including all metabolome analysis. T.H., R.K., M. Yamazaki, T. Oshio, T. Otusbo, K.K., K.I.-O., K. Higuchi, and Y.I.K. carried out experiments including cell separation and histological experiments and data analysis.

Additional information

Accession codes: microarray data have been deposited in the Gene Expression Omnibus database under accession code GSE40370.

Supplementary Information accompanies this paper at http://www.nature.com/naturecommunications

Competing financial interests: The authors declare no competing financial interests.

Reprints and permission information is available online at http://npg.nature.com/reprintsandpermissions/

How to cite this article: Okada, T. *et al.* Microbiota-derived lactate accelerates colon epithelial cell turnover in starvation-refed mice. *Nat. Commun.* 4:1654 doi: 10.1038/ncomms2668 (2013).